

REPORT DOCUMENTATION PAGE
*Form Approved
OMB No. 0704-0188*

The public reporting burden for this collection of information is estimated to average 1 hour per response, including the time for reviewing instructions, searching existing data sources, gathering and maintaining the data needed, and completing and reviewing the collection of information. Send comments regarding this burden estimate or any other aspect of this collection of information, including suggestions for reducing the burden, to Department of Defense, Washington Headquarters Services, Directorate for Information Operations and Reports (0704-0188), 1215 Jefferson Davis Highway, Suite 1204, Arlington, VA 22202-4302. Respondents should be aware that notwithstanding any other provision of law, no person shall be subject to any penalty for failing to comply with a collection of information if it does not display a currently valid OMB control number.

PLEASE DO NOT RETURN YOUR FORM TO THE ABOVE ADDRESS.

1. REPORT DATE (DD-MM-YYYY)				2. REPORT TYPE	3. DATES COVERED (From - To)	
4. TITLE AND SUBTITLE				5a. CONTRACT NUMBER		
				5b. GRANT NUMBER		
				5c. PROGRAM ELEMENT NUMBER		
6. AUTHOR(S)				5d. PROJECT NUMBER		
				5e. TASK NUMBER		
				5f. WORK UNIT NUMBER		
7. PERFORMING ORGANIZATION NAME(S) AND ADDRESS(ES)					8. PERFORMING ORGANIZATION REPORT NUMBER	
9. SPONSORING/MONITORING AGENCY NAME(S) AND ADDRESS(ES)					10. SPONSOR/MONITOR'S ACRONYM(S)	
					11. SPONSOR/MONITOR'S REPORT NUMBER(S)	
12. DISTRIBUTION/AVAILABILITY STATEMENT						
13. SUPPLEMENTARY NOTES						
14. ABSTRACT						
15. SUBJECT TERMS						
16. SECURITY CLASSIFICATION OF: a. REPORT b. ABSTRACT c. THIS PAGE			17. LIMITATION OF ABSTRACT	18. NUMBER OF PAGES	19a. NAME OF RESPONSIBLE PERSON 19b. TELEPHONE NUMBER (Include area code)	

Final report to the
Office of Naval Research

on the

Viscoelastic Material Characterization
relative to Constitutive and Failure Response of an
Elastomer

under the
ONR Research Grant,
No.N00014-03-1-0539,

to the

California Institute of Technology

PI: W. G. Knauss
Program Officer: Dr. R. Barsoum, ONR 334

Graduate Aeronautical Laboratories,
California Institute of Technology
Pasadena, California 91125

Mach 2004

Summary

It was the objective of this program to determine the time-dependent (viscoelastic) response of an elastomer at various temperatures so as to be able to construct the uniform master relaxation response, from which the mechanical responses under a wide range of prescribed load or deformation histories may be deduced at any reference temperature.

This report summarizes work accomplished during the referenced grant. Early efforts were expended on re-establishing test facilities, verifying proper operations and their precision limits. Particular attention was devoted to the precision with which the loads and deformations could be determined. Strain measurements were taken for monitoring purposes by means of the digital image correlation method. Because of the desire to determine also the time dependent Poisson behavior, digital image correlation was attempted in both the axial and transverse directions. While consistent data were obtained for strain monitoring in the axial direction, the precision with which lateral strains could be determined overlong periods of time was not sufficient to specify the volumetric or bulk behavior in the rubbery domain.

The report is divided into several parts, namely a summary of linear viscoelasticity principles, the delineation of the experimental requirements and verification of the test method precision. In this context it is of interest to note that test machine precision was found to be insufficient to prescribe axial strains on the uniaxial specimens of below about 1-2%. However, a 2%-strain prescription was still able to render the essentially linearly viscoelastic behavior of the material.

The time-temperature superposition method provided a master relaxation function for the elastomer and determined its glass transition temperature to be near -50°C. The range of modulus values measured over a temperature-reduced time range of 15 decades varied by a factor of about 12-15. By usual standards of polymer behavior in the transition range this is not a very large variation, though not abnormally small, especially if one considers that the full range of the glass-to-rubber transition has not been captured. Estimates are presented that illustrate the conversion of the measured relaxation response of this material into a different time responses under short term loading at different temperatures.

TABLE OF CONTENTS

1. BACKGROUND

1.1 *Linear Viscoelasticity*

1.1.1 *Specific constitutive responses (isotropic solids)*

1.1.2 *Shear Response:*

1.1.3 *Bulk or Dilatation Response.*

1.1.4 *Uniaxial behavior.*

1.1.5 *Influence of temperature on the viscoelastic time scale*

1.1.5.1 *The entropic contribution:*

1.1.5.2 *Time-temperature tradeoff, the phenomenon.*

1.1.5.3 *The role of the entropic contribution.*

1.1.5.4 *The shift Factor*

1.1.5.5 *Time-Temperature shifting near and below the glass transition.*

1.1.6 *Influence of pressure on the viscoelastic time scale*

1.1.7 *Representation of the relaxation and creep functions*

1.1.8 *General three-dimensional constitutive description.
nonlinearly viscoelastic concepts*

2. MEASUREMENTS OF ELASTOMER PROPERTIES

2.1 *Tools*

2.1.1 *Calibration of load cell*

2.1.2 *Precision of strain prescription (strain vs displacement monitoring)*

2.1.3 *DIC image file size and strain resolution*

2.1.4 *Temperature control and tracking*

2.2 *Properties Determination*

2.2.1 *Specimen configurations (a) relaxation, (b) rupture*

2.2.2 *Loading (straining) programs(s)*

2.2.3 *Relaxation at various temperatures*

2.2.4 *Master relaxation curve*

2.2.5 *Time-temperature shift data*

2.2.6 *Poisson behavior*

2.2.7 *Rupture behavior*

2.2.8 *The influence of pressure on time dependent behavior*

2.2.8.1 *Time-pressure shifting*

2.2.8.2 *Need for data and consequences for subsequent analyses*

3. APPLICATION TO ARBITRARY DEFORMATION HISTORIES

3.1 *Variable Temperature and Pressure*

3.2 *Approximations for Finite Deformations.*

3.3 *Approximations for Monotonically Changing Deformations*

4. REFERENCES

5. ACKNOWLEDGEMENTS

1. BACKGROUND

1.1 LINEAR VISCOELASTICITY

The present investigation was limited to linearly viscoelastic behavior, because (a) the understanding of non-linear material characterization of polymer mechanical behavior is in a poorly developed state and needs much development yet, and (b) there were insufficient resources and time to embark on a drawn-out characterization with the aim to develop non-linearly viscoelastic material characterization. While there are proposed frame works for representing nonlinear material behavior (Schapery 1968, 1969), Emri and Knauss (1981, 1987), they are not in a state of uniformly accepted engineering practice. The framework to describe linearly viscoelastic material behavior used effectively for many years in engineering applications bears phenomenological character. It is based mathematically on either an integral or differential formulation with the material representation described realistically in numerical (tabular) or functional form(s). The fundamental equations governing the linearized theory of viscoelasticity are the same as those for the linearized theory of elasticity, except that the generalized Hooke's law of elasticity is replaced by a constitutive description that is sensitive to the material's (past) history of loading or deformation. It will be the purpose of the immediately subsequent sections to delineate the details of this formalism of material description.

1.1.1 *Specific Constitutive Responses (Isotropic Solids)*

With the subsequent and specific study in mind the following discussion is limited to isotropic materials. Recalling that the stress and strain states may be decomposed into shear and dilatational contributions (deviatoric and dilatational components), we deal first with the shear response for exemplary purposes followed by the volumetric part. Thermal and pressure sensitive characterization will be dealt with at a later time.

1.1.2 *Shear Response:*

Let τ denote any shear stress component and ε^1 its corresponding shear strain. Denote the material characteristic for unit step excitation in the present shear context by $\mu(t)$. This function is identified as the **relaxation modulus in shear**² (for an isotropic material). The constitutive response in a pure shear deformation is the given by

$$\tau(t) = 2 \int_0^t \mu(t-\xi) \frac{d\varepsilon(\xi)}{d\xi} d\xi \quad (1)$$

¹ Standard continuum mechanics notation is consistently implied in this document.

² Relaxation is a phenomenon associated with prescribing a step-wise deformation on a test sample. If the deformation mode is a shear strain, the resulting relaxation modulus is called a shear relaxation modulus. It is defined as the resulting time varying shear stress, normalized by the amplitude of the (step) strain.

$$\begin{aligned}
&= 2\varepsilon(0)\mu(t) + 2 \int_{0^+}^t \mu(t-\xi) \frac{d\varepsilon(\xi)}{d\xi} d\xi \\
&= 2\mu * d\varepsilon
\end{aligned} \tag{2}$$

where the star-notation replaces the integral notation for purposes of brevity and $\mu(t)$ is clearly the relaxation modulus under **unit** step strain input since it follows from (2) that for the step strain history $\varepsilon(t) = \varepsilon_o h(t)$ of amplitude ε_o , the response is

$$\tau(t) = 2\mu(t) \varepsilon_o \tag{3}$$

The complementary (inverse) relation for a prescribed shear stress is

$$\varepsilon(t) = \frac{1}{2} \int_0^t J(t-\xi) \frac{d\tau(\xi)}{d\xi} d\xi \tag{4}$$

$$\begin{aligned}
&= \frac{1}{2} \tau(0) J(t) + \frac{1}{2} \int_{0^+}^t J(t-\xi) \frac{d\tau(\xi)}{d\xi} d\xi \\
&= \frac{1}{2} J * d\tau
\end{aligned} \tag{5}$$

where now the function **J(t)** is the **shear creep³ compliance**, which represents the creep response of the material in shear under application of a step shear stress of unit magnitude.

1.1.3 Bulk or Dilatation Response.

Let $\varepsilon_{ii}(t)$ represent the first strain invariant and $\tau_{jj}(t)$ the corresponding stress invariant. The latter is recognized as three times the pressure $P(t)$, *i.e.* $\tau_{jj}(t) \equiv 3P(t)$. In completely analogous fashion to equations 1 and 2 the bulk behavior, governed by the **bulk relaxation modulus k(t)** is represented by

$$\sigma_{jj}(t) = 3 \int_0^t k(t-\xi) \frac{d\varepsilon_{ii}(\xi)}{d\xi} d\xi \tag{6}$$

$$\begin{aligned}
&= 3\varepsilon_{ii}(0)k(t) + 3 \int_{0^+}^t k(t-\xi) \frac{d\varepsilon_{ii}(\xi)}{d\xi} d\xi \\
&= 3k * d\varepsilon_{ii}
\end{aligned} \tag{7}$$

The inverse relation is, similarly,

$$\varepsilon_{ii}(t) = \frac{1}{3} \int_0^t M(t-\xi) \frac{d\sigma_{jj}(\xi)}{d\xi} d\xi \tag{8}$$

³ Creep is the time dependent strain response of a test body to the prescription of a time-invariant stress. The creep function is a monotonically increasing function of time.

$$\begin{aligned}
&= \frac{1}{3} \sigma_{jj}(0) M(t) + \frac{1}{3} \int_{0^+}^t M(t-\xi) \frac{d\sigma_{jj}(\xi)}{d\xi} d\xi \\
&= \frac{1}{3} M * d\epsilon_{ii}
\end{aligned} \tag{9}$$

where the function **M(t)** represents now the **dilatational creep compliance** (also called the bulk creep compliance), or, in physical terms, the time dependent fractional volume change resulting from the imposition of a unit step pressure.

1.1.4 Uniaxial behavior.

It is very common in engineering descriptions to work with the uniaxial characterization commensurate with the use of Young's modulus in linear elasticity. If one defines **E(t)** as the relaxation modulus characterizing the uniaxial stress response to a step strain input of unit magnitude, then the stress response, say $\sigma_{11}(t)$ following a uniaxial step strain history $\epsilon_{11}(t)$ is given, in complete analogy to equations (1-2) as

$$\sigma_{11}(t) = \int_0^t E(t-\xi) \frac{d\epsilon_{11}(\xi)}{d\xi} d\xi \tag{10}$$

$$\begin{aligned}
&= \epsilon_{11}(0) E(t) + \int_{0^+}^t E(t-\xi) \frac{d\epsilon_{11}(\xi)}{d\xi} d\xi \\
&= E * d\epsilon_{11i}
\end{aligned} \tag{11}$$

with the corresponding inverse relation

$$\epsilon_{11}(t) = \int_0^t D(t-\xi) \frac{d\sigma_{11}(\xi)}{d\xi} d\xi \tag{12}$$

$$\begin{aligned}
&= \sigma_{11}(0) D(t) + \int_{0^+}^t D(t-\xi) \frac{d\sigma_{11}(\xi)}{d\xi} d\xi \\
&= D * d\sigma_{11i}
\end{aligned} \tag{13}$$

where the monotonically increasing function **D(t)** is called the uniaxial creep compliance is the measure of how rapidly the uniaxial strain increases with time under the imposed unit-sized step stress $\sigma_{11} = h(t)$. These relations are often represented with the help of mechanical analog models shown in figure 1 as described later on.

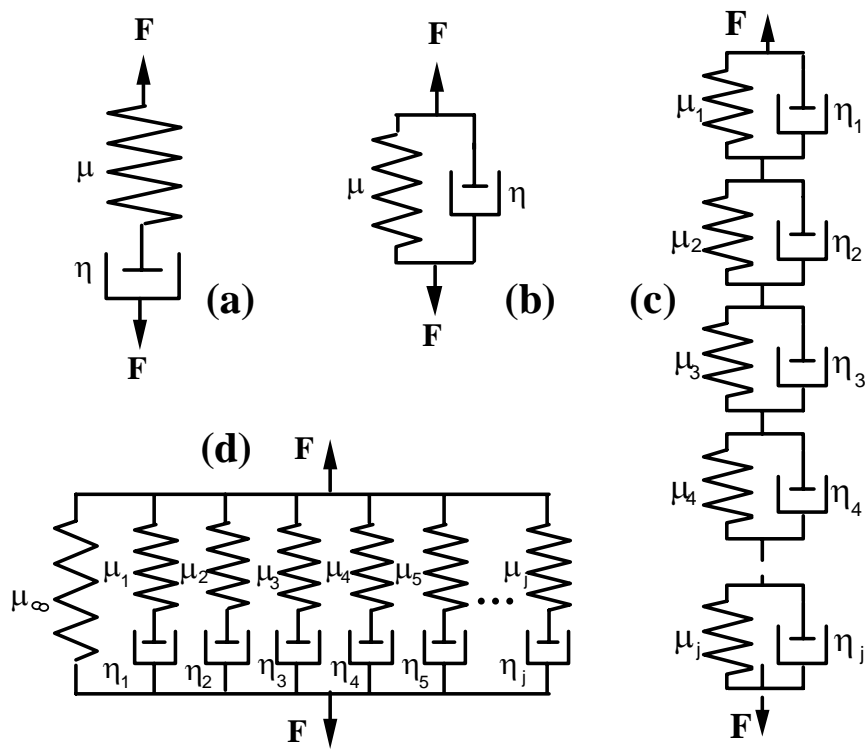


Figure 1. Several analog models used historically in representing linearly viscoelastic material response.

1.1.5. *Influence of temperature on the viscoelastic time scale*

Temperature is one of the most important environmental variables to affect polymers in engineering use, primarily because normal use conditions are relatively close to the material characteristic called the glass transition temperature – or “glass temperature” for short. In parochial terms –a closer definition follows- the glass temperature signifies the thermal range in which the material changes from a stiff or hard material to a soft or compliant one. The major effect of the temperature, however perceived by the user, is through its influence on the creep or relaxation time scale of the material.

Solids other than polymers also possess characteristic temperatures, as, *e.g.* the melt temperature in metals; for polymers the melt temperature signifies melting of crystallites in the (semi-) crystalline variants. Also, typical amorphous solids like silicate glasses and amorphous metals, exhibit distinct glass transition temperatures; indeed, much of our understanding of glass transition phenomena in polymers originated in understanding related phenomena in the context of silicate glasses.

1.1.5.1 The entropic contribution:

Among the long-chain polymers, elastomers⁴ possess a molecular structure that comes closest to our idealized understanding of molecular interaction. The connection between the molecular motion under forces applied external to the network can be provided through thermodynamic reasoning. In this way the “classical” constitutive behavior under moderate deformations (up to about 100% strain in uniaxial tension) has been formulated by Treloar in 1958⁵. In the present context the role of the temperature is

of primary interest and it suffices, therefore, to quote his results in the form of the constitutive law for an incompressible solid (constant density). Of particular importance is the dependence of the stress on the material property which relation is for the uniaxial tension state (say, in the 11-direction)

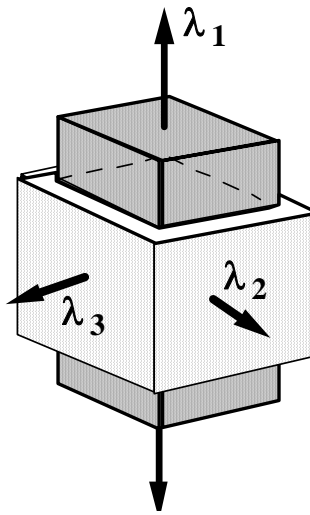


Figure 2: Deformation of a cube into a parallelepiped. The unit cube sides have been stretched orthogonally in length to the extension or stretch ratios λ_1 , λ_2 , and λ_3 .

$$\sigma = \frac{1}{3} N k T \left\{ \lambda_1^2 - \frac{1}{\lambda_1} \right\} \quad \text{subject to} \quad \lambda_1 \lambda_2 \lambda_3 = 1 \quad (20)$$

where λ_1 , λ_2 and λ_3 denote the (principal) extension ratios of the deformation illustrated in figure 2 (though only for the condition $\lambda_1 \lambda_2 \lambda_3 = 1$), and the multiplicative factor consists of the number of chain segments between crosslinks, N , Boltzmann’s constant k and the absolute temperature T . Since for infinitesimal deformations $\lambda_1 = 1 + \varepsilon_{11}$, *i.e.* the extension ratio differs from unity by the small axial strain ε_{11} , one finds upon expanding (20) in terms of strains small relative to unity that $N k T$ must equal the elastic Young’s modulus

⁴ “Elastomer” is an alternative name for rubber, a cross-linked polymer, possessing a glass transition temperature that is considerably below normal environmental conditions. Molecule segments are freely mobile relative to each other except for “being pinned” at the cross-link sites

⁵ Because this constitutive formulation involves the entropy of a deformed rubber network, this temperature effect of the properties is usually called the “entropic” temperature effect.

E_∞ . It is thus established that the (small-strain) Young's modulus is directly proportional to the absolute temperature, and that this holds also for the shear modulus because, under the restriction/assumption of incompressibility ($\lambda_1\lambda_2\lambda_3=1$) the shear modulus μ_∞ of the rubber equals $1/3 E$, *i.e.* $\mu_\infty = \frac{1}{3} E_\infty$. Thus $\mu_\infty/T = Nk$ is a material constant, from which it follows that comparative moduli obtained at temperatures T and T_0 are related by

$$\mu_\infty|_T = \frac{T}{T_0} \mu_\infty|_{T_0} \quad \text{or equivalently} \quad E_\infty|_T = \frac{T}{T_0} E_\infty|_{T_0} \quad (21)$$

1.1.5.2 Time-temperature tradeoff, the phenomenon.

A much more significant influence of temperature on the viscoelastic behavior is experienced in connection with the time scales under relaxation or creep. To set the proper stage we define first the notion of the glass transition temperature T_g . To this end consider a measurement of the specific volume as a function of temperature. Typically, such measurements are made in a setting where the temperature decreases “slowly”, since

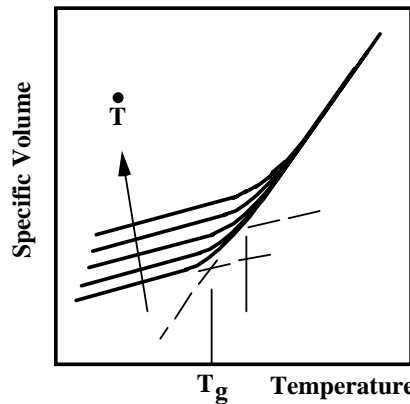


Figure 3. A typical set of measurements of specific volume as a function of temperature under variable cooling rates.

the rate of cooling has an influence on the outcome. Figure 3 shows a typical result, which illustrates that at sufficiently low and high temperatures the volume dependence is linear, with a transition connecting the two segments. The glass transition temperature is defined as the intersection of two linear extensions of the two segments roughly in the center of the transition range. As also indicated in that figure, an increase in the rate of cooling causes reduced volume shrinkage as a result of the unstable evolution of a molecular microstructure that consolidates with time. This phenomenon is associated with physical ageing. In practical terms the lowest –most stable- response curve is determined basically by the patience of the investigator, though substantial deviations must be measured in terms of logarithmic time units: Thus, relatively little may be gained by reducing the cooling rate from one to a tenth of a degree centigrade per hour.

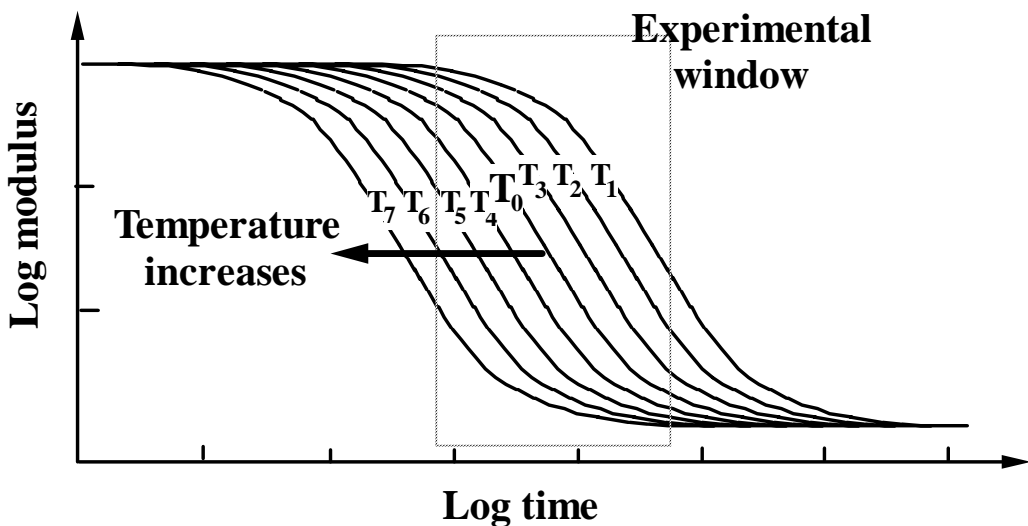


Figure 4: Idealized presentation of relaxation behavior at various temperatures T_0 — T_7 .
 Scale markers represent a decade. The “experimental window” represents a typical time range available for a measurement sequence.

We turn next to **the most important effect of temperature on the time scale** and present this phenomenon in terms of a relaxation response, say in shear. The discussion is generic in the sense that it applies, to the best of the collective scientific knowledge, to all time and rate sensitive properties, at least for polymers⁶ For ease of presentation we ignore first the entropic temperature effect discussed above and impose no constraint on the applicable temperature range. Moreover, we limit ourselves to considerations above the glass transition temperature, with discussion of behavior around or below that temperature range reserved for later amplification. This limitation is consistent with the behavior of the elastomer considered in this study as illustrated later on.

Figure 4 shows a series of relaxation curves measured at different temperatures in an ideal test situation. Accordingly, increasing temperatures shift the relaxation behavior to shorter times parallel to the logarithmic time axis. This logarithmic shift corresponds thus to a multiplicative factor that depends on the temperature.

In reality experimental constraints do not allow the full range of relaxation to be measured at any one temperature. Instead, measurements can typically be made only within the time frame of a certain “test window” indicated by the dashed outline in figure 4. Accordingly, the more realistically acquired data would appear as indicated in figure 5. If one accepts this “time-temperature equivalence” and the associated “time-temperature shift” process, then a single curve —the master curve— may be constructed from the segments in this figure by shifting the temperature segments with respect to one obtained at a temperature that may be chosen arbitrarily, so as to construct the master curve corresponding to that

⁶ The technological evolution of metallic glasses is relatively recent, so that a limited amount of data exists in this regard.

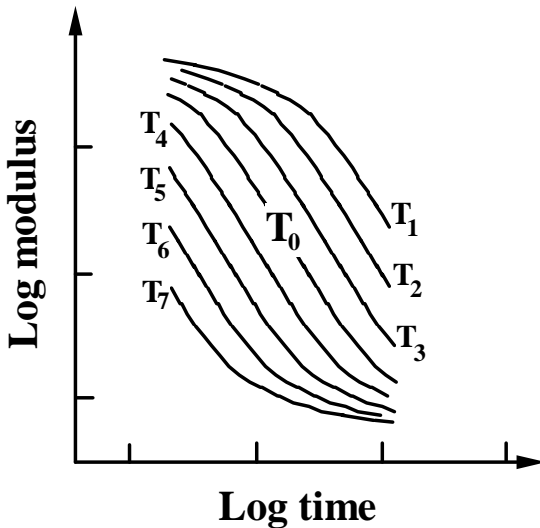


Figure 5: Simulation of typical data acquired at various temperatures.

from which the segments would have been deduced according to the scheme in figure 4. Because this time-temperature trade-off has been deduced from physical measurements without the benefit of a time scale of unlimited extent, the assurance that this “shift-process” is a physically acceptable or valid scheme can be derived only from the quality with which the “shifting” or “superposition” can be accomplished. To examine this quality issue requires that test temperatures are chosen sufficiently closely, and that the measurements vary widely enough over the log-time range to afford considerable overlap of the shifted curve segments.

In this construction a composite curve develops, termed the “master curve”, as the curve segments are shifted relative to one obtained at some arbitrarily chosen temperature. At the same time the amount of shift along the log-time axis is recorded as a function of the temperature. This function, usually called the “temperature dependent shift factor”, or simply “shift factor” for short, is a material characteristic, and is often designated by the symbol ϕ_T . Figures 7 and 8 illustrate the application of the shift principle for a polyurethane elastomer (Thiokol Solithane 113, 50/50 composition), together with the associated shift factor ϕ_T in figure 7 with the inclusion of the entropic effect.

1.1.5.3 *The role of the entropic contribution.*

Having demonstrated the “shift-phenomenon” in principle, it remains to address the effect of the entropic contribution to the time dependent master response. Recall that the entropic considerations were derived in the context of purely rubbery material behavior, and specifically in the absence of viscoelastic effects. Thus any modulus variation with

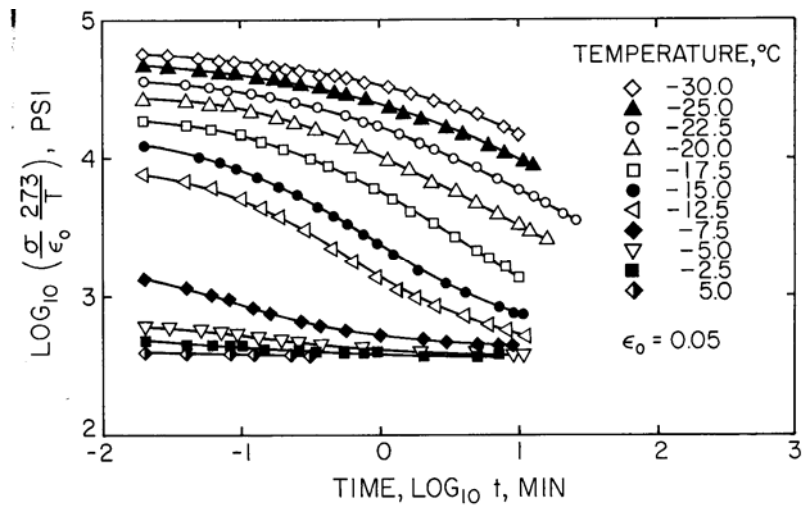


Figure 6: Relaxation modulus for a Polyurethane formulation measured at various temperatures in uniaxial tension.

temperature is established, strictly speaking, only in the long term time domain when rubbery behavior dominates, so that equations (21) apply. Various arguments have been put forward to apply a similar reduction scheme to data in the viscoelastic transition region. Two arguments dominate, but they are based on pragmatic rather than rigorously scientific principles. The first argument states that even in the transition region the polymer chain segments experience locally elastic behavior in accordance with the theory of rubber elasticity. Accordingly, all curve segments obtained at the various temperatures should be multiplied by their respective ratios of the reference temperature and the test temperature, *i.e.* T_0/T , in the case of modulus measurements, and with the inverse ratio in the case of compliance measurements, regardless of by how many log-time units the material behavior is removed from the rubbery long-term domain. The alternative view asserts that the entropic correction does not apply in the glassy state and, accordingly should decrease continuously from the long-term, rubbery domain as the glassy or short-term behavior is approached. The rule by which this change occurs is not established scientifically either, but is typically taken to be linear with the logarithmic time scale throughout the transition. Ultimately, the precision of the data and its treatment needs to decide as to whether one or the other scheme produces the “better master curve” by the argument as to which procedure provides the best overlap of the data. Historically, the first scheme has been practiced more frequently than the latter.

In the present study it turned out that the material behavior was accessible mostly in the near-rubber domain, only so that the first of the above reduction schemes was applied.

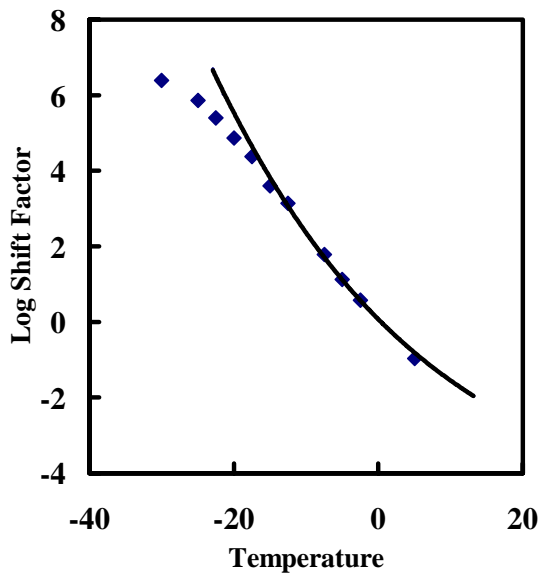


Figure 7: Time temperature shift factor for reducing the Polyurethane data in figure 7 to that in figure 9. $T_g = -18^\circ\text{C}$. The solid line represents the WLF – equation

$$\text{Log}_{10}\phi_T = \frac{-8.86(T - 32^\circ\text{C})}{101.6 + (T - 32^\circ\text{C})} - 4.06$$

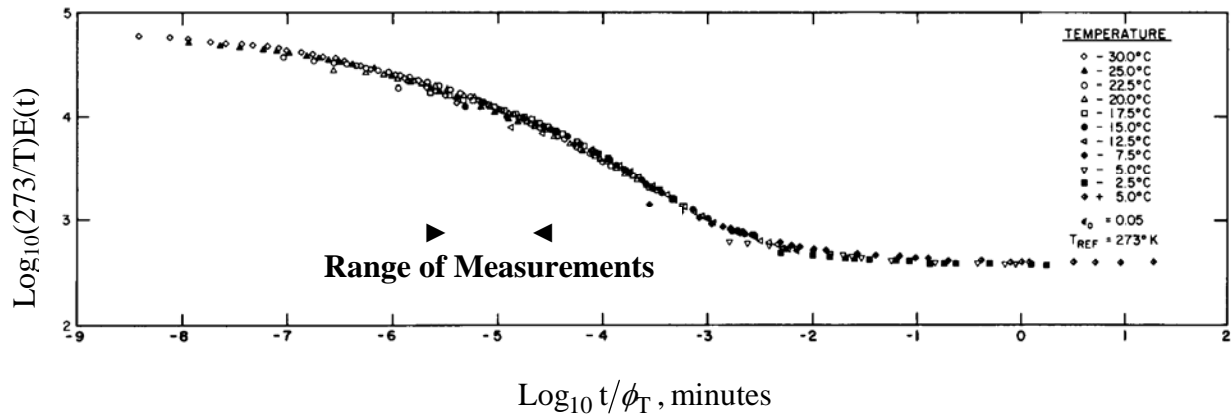


Figure 8: Temperature reduced uniaxial relaxation modulus (Master curve) for a Polyurethane formulation derived from data in figure 6 and with the shift factors in figure 7.
Reference to “Range of Measurements” pertains to discussion in the text.

1.1.5.4 *The temperature shift factor*

While several researchers have contributed significantly to clarifying the concept and the importance of the time-temperature superposition principle, it was the group of Williams, Landel and Ferry (1955) that has been credited with formulating the time-temperature relationship through the now ubiquitously quoted WLF equation: they demonstrated the near universality of this connection for many diverse polymers, and provided a physical model for the process in terms of a free-volume interpretation. Plazek (1965) has supplied an exemplary demonstration of the nearly perfect obeyance of the “shift phenomenon” for Polystyrene. Ignoring, for brevity of presentation, the polymer mechanical argumentation, Williams, Landel and Ferry (1955) suggested that above the glass transition temperature the shift factor is given in functional form by the relation

$$\log[a_T] = \frac{c_1(T - T_{ref})}{c_2 - (T - T_{ref})} \quad (22)$$

where T_{ref} denotes a reference temperature typically about 50 °C above the glass transition temperature of the polymer under consideration. The constants c_1 and c_2 vary from polymer to polymer, but for many take on values around $c_1 \sim 8.86$ and $c_2 \sim 101.6$. It is of interest to note, but of no particular consequence for the purposes of this summary that the same functional relation can be derived starting from thermodynamic reasoning without any recourse to the arguments offered by Williams, Landel and Ferry. As a consequence one must consider, in principle, either derivation questionable, and the physical basis of equation (22) as ultimately unsettled and thus, as yet, empirical.

An illustration of data reduction employing the entropic correction (applied over the whole transition range) and the time-temperature superposition of measured data is given in figures 6-8. Figure 6 presents tensile relaxation data for a polyurethane elastomer, possessing a glass transition temperature of -18 °C, as measured at different temperatures. Shifting the curve segments relative to the 0 °C data by the shift factor shown in figure 7 produces the master curve in figure 8. Because the data segments were shifted relative to the data obtained at 0°C, the master curve represents relaxation behavior at that temperature. Data at different temperatures may then be deduced with the help of the shift factor in figure 7.

1.1.5.5 *Time-Temperature shifting near and below the glass transition.*

The time temperature shifting above the glass transition has been presented as basically an empirical rather than uniquely explained process, though many researchers firmly trust its validity because of extensively consistent demonstration. The applicability of the shift principle to temperatures near and below the glass transition has been questioned for many years, but is gradually gaining acceptance with certain provisos. First, no functional analytic form has been proposed –unique or conflicting- that yields credence to the effect in terms of some molecular model.

Moreover, because phenomena at and below the glass transition do not occur with molecular conformation being in equilibrium, the ideas underlying the shift phenomenon above the glass transition are questioned more readily, because the role of dilatation interferes with simple concepts and complicates the rules by which such examinations and data interpretations are carried out. For example, Losi and Knauss have argued on the basis of free volume considerations that any shift operation below the glass transition should depend on the temperature rate with which the state of the polymer is approached, slower rates leading to a “more unique” adherence to a shift concept. Many independent, though not necessarily thoroughly documented counterparts have been produced over the last decade that present equally supportive information of a consistent time-temperature superposition application through and below the glass transition.

1.1.6 *Effect of Dilatation on Creep and Relaxation Times (Pressure effects)*

An important consequence of free volume consideration is reflected in the behavior of polymers under high pressures. In section 4.4 it was noted that the WLF equation (22) can be derived using argumentation based on the role of free volume. That reasoning asserts that an increase in the space around molecule increases the ability and speed of molecule segments to adjust to new positions relative to each other in the process of relaxation or creep. While this idea has been considered mostly in connection with pressure superposed on a tensile or shear deformation, it should be equally applicable to situations involving positive dilatation. This concept has been investigated by only a few investigators, but even so an exhaustive presentation of these results is beyond the scope of the present objective. However, this concept plays a significant role in the discussion of fracture and stress wave propagation. Stated as a general thermoelastic concept by Ferry it has been explored experimentally by Fillers and Tschoegl (1977), Moonan and Tschoegl (1985), who studied the effect of pressure on the relaxation times in the rubbery domain, and by Knauss and Emri (1981, 1987) and by Losi and Knauss (1992) in the formulation of dilatation induced nonlinearly viscoelastic behavior for structural polymers. The most recent confirmation of this phenomenon or viscoelastic feature is a study by Qvale and Ravi-Chandar (2004) which addresses viscoelastic property measurements on PMMA and PC.

The net result of these investigations is that the dilation, whether positive or negative, has an effect on the material time scale similar—if not identical—to a lowered or raised temperature, respectively. Moreover, as is the case of the temperature induced shift phenomenon for which the free-volume model of the shift factor, equation (22), was deduced by Williams, Landel and Ferry, the magnitude of the dilatation necessary to effect significant changes in the relaxation or creep time scales may be very small, *i.e.*, on the order of only 10^{-3} or less. With regard to failure and /or shock wave environments this is an important observation because at the tip of a crack the high stresses are thus automatically a source of shift in time response in the material. This notion appears to be particularly important for the fracture of structural polymers because the high crack tip stresses dominate and accelerate the viscoelastic yield-like behavior of the materials in the region where fracture occurs. With respect to the propagation of pressure waves this notion

implies an automatic shift of the relaxation or creep spectrum to the more dissipative region of the spectrum if an elastomer is involved such as is the topic of this investigation. Associated with this shift to higher dissipation an apparent stiffening of the material is experienced.

1.1.7 Representation of the Relaxation and Creep Functions (Spectra and functional representation)

Various mathematical forms have been suggested and used to represent the material property functions. Preferred forms have evolved with precision being balanced against ease of mathematical use or minimum number of parameters required. All viscoelastic material functions possess the common characteristic that they vary monotonically with time: relaxation functions decrease and creep functions increase monotonically. A second characteristic of realistic material behavior is that time is (almost) invariably measured in terms of (base10) logarithmic units of time.

Early representations of viscoelastic responses were closely allied with (simple) mechanical analog models (Kelvin, Voigt) or their derivatives. Without delving into the details of this evolutionary process, their generalization to broader time frames lead to the “spectral representation” of viscoelastic properties, so that it is useful to present only the rudiments of that development. The “building blocks” of the analog models⁷ are the Maxwell and the Voigt models illustrated in figure 1a and 1b. Under a step-wise applied deformation of magnitude ε_0 —represented by the separation of the force-application points in the Maxwell model, Figure 1a— the stress (force) abates or relaxes by the relation

$$\tau(t) = \varepsilon_0 \cdot \exp(-t/\xi) \quad (14)$$

where $\xi = \mu_m / \eta_m$ is called the relaxation time. Similarly, applying a step stress (force) of magnitude τ_0 to the Voigt element (Figure 1b) engenders a time dependent separation (strain) of the force-application points described by

$$\varepsilon(t) = \frac{\tau_0}{\mu} [1 - \exp(-t/\zeta)] \quad (15)$$

where $\zeta = \mu_v / \eta_v$ is now called the retardation time since it governs the rate of retarded or delayed motion. Note that this representation is symbolic for illustration purposes here and that the retardation time for the Voigt material is not necessarily meant to be equal to the relaxation time of the Maxwell solid. In fact, in general relaxation times are not equal to

⁷ Force $F \sim$ stress τ and deformation $\delta \sim$ strain ε .

retardation times. The relaxation modulus and creep compliance commensurate with equations 14 (Maxwell model) and 15 (Voigt model) for the Wiechert and Kelvin models (Figures 1c and 1d) are, respectively

$$\mu(t) = \mu_\infty + \sum_n \mu_n \exp(-t/\xi_n) \quad (16)$$

and

$$J(t) = J_g + \sum_n \frac{1}{\mu_n} \left[1 - \exp(-t/\xi_n) \right] + \eta_o t. \quad (17)$$

Here J_g and η_o arise from letting $\eta_1 \rightarrow 0$ (the first Voigt element degenerates to a spring) and $\mu_n \rightarrow 0$ (the last Voigt element degenerates to a dashpot). These series representations with exponentials are often referred to as Prony series.

As the number of relaxation times increases indefinitely, the generalization of the expression for the shear relaxation modulus, becomes

$$\mu(t) = \int_0^\infty H(\xi) \exp(-t/\xi) \frac{d\xi}{\xi} \quad (18)$$

where the function $H(\xi)$ is called the “distribution function of the relaxation times”, or relaxation spectrum, for short; the creep counterpart presents itself with the help of the retardation spectrum $L(\zeta)$ as

$$J(t) = J_g + \int_0^\infty L(\zeta) [1 - \exp(-t/\zeta)] \frac{d\zeta}{\zeta} + \eta \cdot t. \quad (19)$$

Note that although the relaxation times ξ and the retardation times ζ do not, strictly speaking, extend over the range from zero to infinity, the integration limits are so assigned for convenience since the functions $H(\xi)$ and $L(\zeta)$ can always be chosen to be zero in the corresponding part of the infinite range.

A typical example of a relaxation modulus, say in shear (or in uniaxial tension) is illustrated in figure 8. It is particularly noteworthy that the time scale ranges over many decades which are typically very difficult or impossible to access directly in a standard laboratory environment. It is the subject of this report to display this complete time scale on the basis of the Time-Temperature Tradeoff principle, as discussed below. While we have chosen to perform this characterization in terms of the relaxation phenomenon, it should be stated that other laboratories might perform this task in terms of so-called dynamic or complex environment. This mode is not discussed here, though interrelations can be derived immediately from equations (1-13).

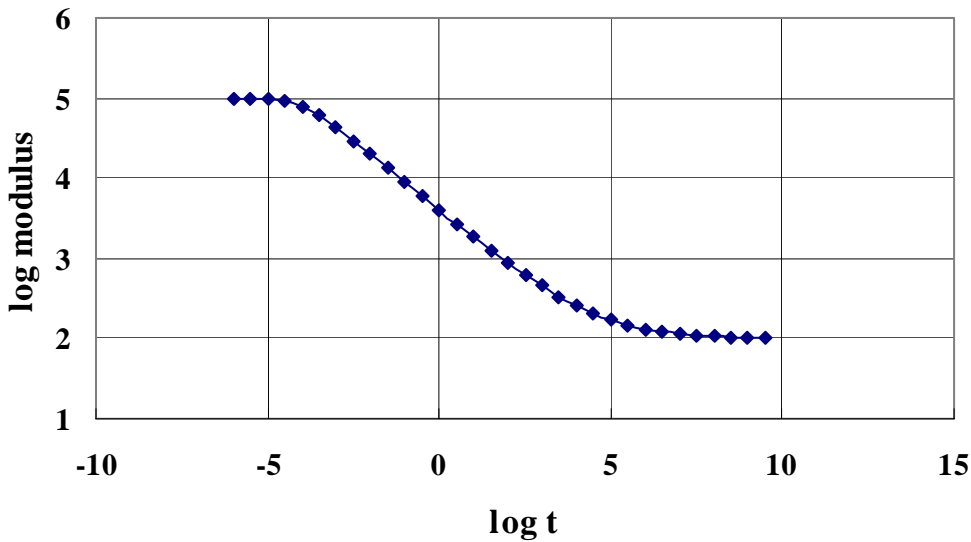


Figure 9: Example of a typical relaxation modulus function.

1.1.8. General Three-Dimensional Constitutive Description.

In sections 2.7.2.3 through 2.7.2.5 we have dealt with one-dimensional relations between stress and strain components. We now generalize these descriptions for fully three-dimensional interactions between stresses and strains. We do this here only for isotropic material description and observe that in the limit of vanishing viscoelasticity, *i.e.* for purely elastic behavior, the constitutive laws need to revert to their elastic counterparts. This representation, as illustrated so far for one-dimensional descriptions, essentially replaces the elastic constants by the convolution operators. One notes further that elastic isotropy requires two independent material constants for a complete material characterization. Because in the limit of elastic behavior the viscoelastic response must revert to elastic behavior, it stands to reason that isotropic viscoelasticity requires two independent material functions for a full characterization⁸. Formulating the full constitutive response is most readily accomplished in terms of the deviatoric (shear) and bulk (volumetric) property functions $\mu(t)$ and $k(t)$. Bearing in mind that for three-dimensional problems the stress and strain are function of both space \mathbf{x} ($=x_1, x_2, x_3$) and time t , the isotropic linearly viscoelastic solid constitutive formulation is then, in terms of the deviatoric and dilatational representation,

$$S_{ij}(\mathbf{x}, t) = \int_0^t \mu(t' - \xi') \frac{\partial e_{ij}(\mathbf{x}, \xi)}{\partial \xi} d\xi \quad (23)$$

⁸ This argument clearly does not constitute a proof.

$$\tau_{ii}(\mathbf{x}, t) = 3 \int_0^t k(t' - \xi') \frac{\partial [e(\mathbf{x}, \xi) - \alpha \Delta T(\mathbf{x}, \xi)]}{\partial \xi} d\xi \quad (24)$$

where use has been made of the general, temperature reduced time t' and ξ' ; a time- or rate-independent volumetric coefficient of thermal expansion α has been assumed for ease of presentation. If a history-dependent coefficient of thermal expansion is involved then $\alpha \Delta T$ must be replaced by a convolution equation. Because the integration variable is ξ and not ξ' which depends on ξ , these integrals are not Duhamel or convolution integrals. Nevertheless, we shall use the short notation of the star operation and write, in the absence of thermal expansions,

$$S_{ij}(\mathbf{x}, t) = \mu^* d\epsilon_{ij}(\mathbf{x}, \xi) \quad (25)$$

$$\text{and} \quad \tau_{ii}(\mathbf{x}, t) = 3k^* d\epsilon_{kk}(\mathbf{x}, \xi). \quad (26)$$

Alternate forms in terms of the non-deviatoric stress and strain components are then, without the thermal expansion components

$$\tau_{ij}(\mathbf{x}, t) = 2\mu^* d\epsilon_{ij}(\mathbf{x}, \xi) + \delta_{ij}(k^{-2}/3 \mu)^* d\epsilon_{kk}(\mathbf{x}, \xi) \quad (27)$$

where $\mu(t)$ and $k(t)$ represent the shear and the bulk moduli described in sections 2.1 —2.

Equivalently, one can define the constitutive behavior in terms of the Lamé form if the elastic Lamé parameter λ is considered ~~to be~~ a viscoelastic function so that

$$\tau_{ij}(\mathbf{x}, t) = \lambda^* d\epsilon_{kk}(\mathbf{x}, \xi) \delta_{ij} + 2\mu^* d\epsilon_{ij}(\mathbf{x}, t). \quad (28)$$

Interconnections between $\lambda(t)$ and the other moduli may be deduced, but are not of immediate consequence.

2. MEASUREMENTS OF ELASTOMER PROPERTIES

Having reviewed the general principles of linear viscoelasticity, we turn next to the determination of the viscoelastic characteristics of the elastomer at hand. Following an analysis of the measurement precision for reasons of demonstrating the reliability of the measured functions, we document the master curve(s) for the elastomer, along with a detailed description of the thermo-mechanical trade-off between time and temperature, so that application of the data can be made in any thermal environment.

2.1 Tools.

The viscoelastic characterization was accomplished through measuring the relaxation behavior in uniaxial extension. Such measurements require the recording of the force on a

tensile coupon as a function of time resulting from a “rapidly” applied strain that is held constant with time. Such measurements are in principle readily accomplished with the aid of a (servo-) hydraulic tensile tester (MTS). Though alternate straining devices can be constructed for greater precision in strain definition, this mode was chosen to minimize the time and expense for the overall test program.

2.1.1 Calibration of load cell

The tests were performed on an MTS load unit Model # 358.1 with an axial load transducer by Interface, Model # 1500 ASK-200 having a capacity of 200 lbf. The controller was the installed TestStar II^m system relying on Model 793.00 system software.

Prior to starting test the load cell was calibrated statically with calibrated weights. Since the load range of the load cell extended to 200 lbs and the lowest load measured in the relaxation tests was on the order of 15 lbs, tensile loads could be determined to a fraction of a percent, which was consistent with the error adhering to the determination of the strains (see later).

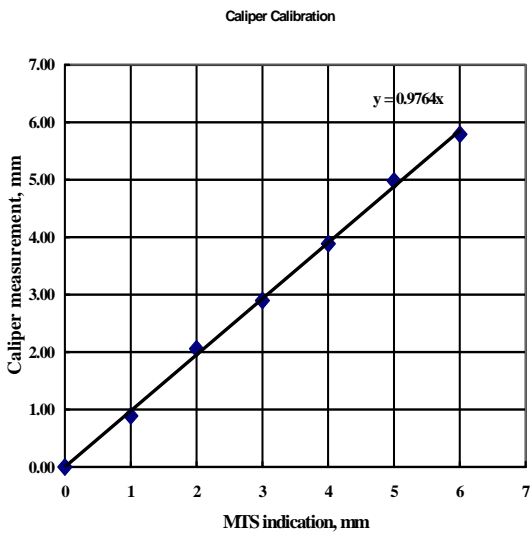


Figure 10: Calibration of the crosshead motion of the MTS machine Against the gage strain measured with calipers.

2.1.2 Test Strain Magnitude

Because it was anticipated initially that measurements would be conducted into the glassy domain for which ancillary studies by Lu and Knauss (1999), and by Knauss and Zhu (2002, 2003) had shown that nonlinear behavior can be encountered at strains of only half a percent, it was desired to employ strains on that order. However, it turned out that the

precision of the servo-controller of the test machine was smaller than stated and anticipated. Many tests had been performed with spurious results which at times indicated that physical properties changed with time and under repeat use in an apparently systematic manner. It was only after a careful calibration of this control capability and after numerous uncertain and spurious variations that the error was cleared up. As a consequence of this finding, the strain amplitude for the relaxation tests needed to be increased. However, it was judged that the penalty of exceeding the possibly nonlinear range was minor compared to the need for sufficient precision. The penalty concern was largely eliminated when it was found at the end of the measurements that the elastomer never entered into the glassy domain, but remained in the near rubbery region where the range of linear behavior is significantly larger than in the glassy domain. After the change to larger strain values was made, all measurements became systematic and in accordance with expected viscoelastic behavior.

2.1.3 Precision of strain prescription (strain vs. displacement monitoring)

It was desired to determine both the axial and the lateral strain in the specimens under load. To this end the Digital Image Correlation (DIC) method was employed, specifically so as to be able to estimate the lateral strain (change). It ultimately turned out that the precision of that method at the strain amplitudes used was insufficient to allow an estimation of a more than nominal Poisson effect to be determined. Thus while the data of this quantity was recorded as matter of routine, the result is essentially that a (near-) incompressible behavior was found (Poisson's ratio $\nu \sim 0.5$). For the axial strain determination the use of the servo-hydraulic test machine required really prescription of the length change of the specimen. To this end a test series was performed in which the routinely and consistently gripped specimen would be extended by recorded amounts. The strain in the specimen test section was recorded by measuring the separation of scribe marks. In addition, the axial strain was determined by the DIC method, and the strain was plotted as a function of the test ram displacement as indicated on the instruments monitoring the test machine. Figure 10 shows the relation between the test frame supplied displacement and the test section strain. This relation was used as a guide in configuring tests, yet, ultimately, the directly measured strain (via DIC) was used for data reduction.

A note is in order on the method employed here for the determination of the strains by means of DIC. In principle DIC is able to determine simultaneously displacements as well as (two-dimensional) strain fields. This capability of DIC is welcome when inhomogenous strain fields prevail. However, when the strain field is homogeneous it has turned out in our past experience that the precision of the strain is increased if the DIC deduced displacements are processed separately for calculating the strain, at the expense of considerable additional time investment. However, it was felt that for this program it was desirable to maximize precision over quantity or speed of data acquisition, so that the more intensive and slower process was chosen.

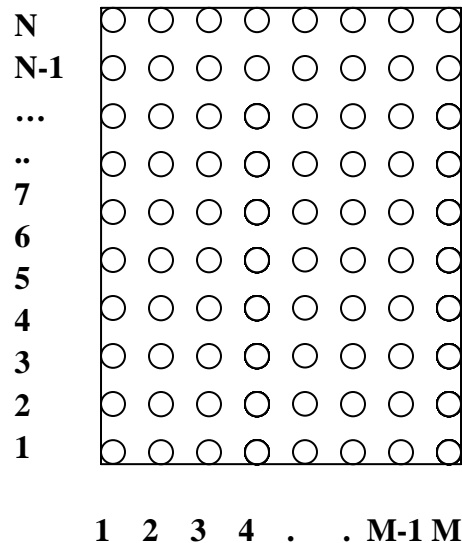


Figure 11: Roster of the centers of image regions within which displacements were determined by means of the DIC method.

To describe the strain determination refer to Figure 11 in which numbers along the ordinate and along the abscissa represent the centers of small domains or image regions around which displacements (and strains) were determined by the DIC method. Because the deformations in a uniaxial strain situations are homogeneous the y-displacements (v) were averaged across the roster (left to right: $m=1$ -to- M) for each line $n=1$ -to- N parallel to the abscissa; subsequently, these x-averaged values were plotted (Excel) against the ordinate number and this essentially linear relation was then fitted with a least-square straight line (also Excel) with the slope being the desired strain. An example plot of this type is shown in Figure 12. We have also explored averaging the DIC determined strains instead of proceeding via the displacements, yet determined that the chosen method was somewhat advantageous over the averaging method.

2.1.4 DIC image file size and strain resolution

In an attempt to improve the resolution of the DIC method for an improved acquisition of the lateral strains a camera of higher pixel count was used for comparison purposes. To this end several comparison measurements were executed with a 3.3 Megabite camera (Nikon Coolpix 995) and a 5.4 Megabite counterpart (Nikon DX1). One might expect from first principles that a higher pixel-per-mm count should lead to a higher precision in the strain resolution, yet such was not clearly the case by the DIC method through which strains were determined. The demonstration of that fact is illustrated in Figure 13. Whether the strain accuracy were to improve through the use of higher pixel density in the range available if the DIC method was used directly to deduce the strain was not explored, since

the present “optimal” method yielded no improvement for the strain extraction.

485-487-5MM-0c

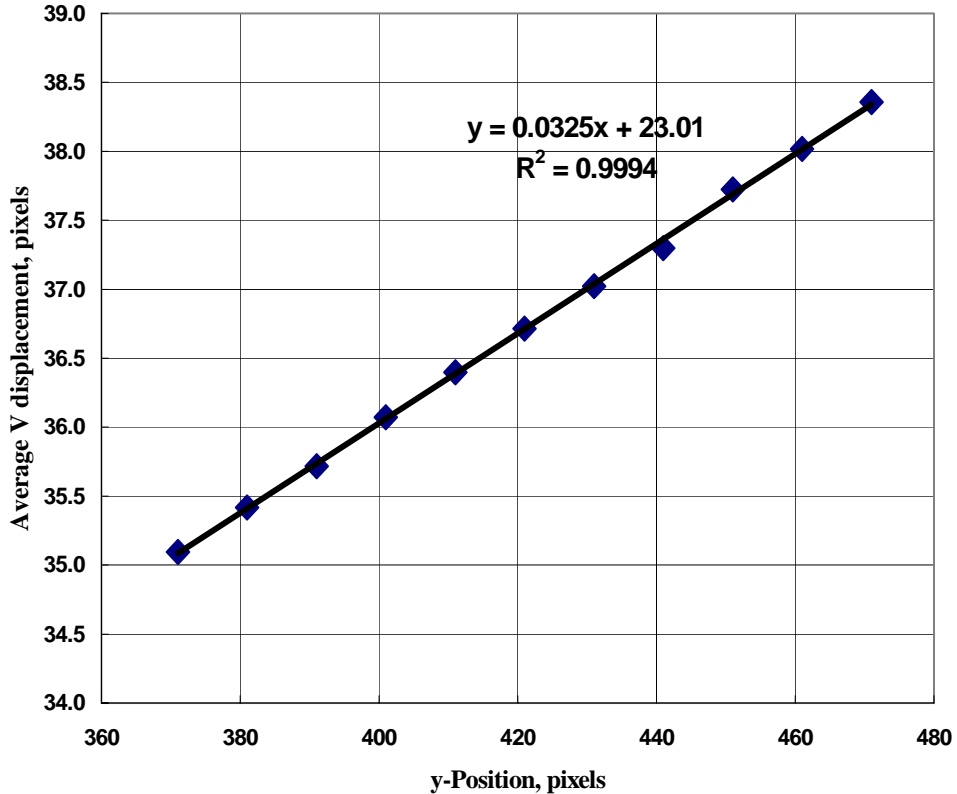


Figure 12: Illustration of the data fit from the DIC method for determining the axial strain (=3.25 % in this example).

For the record it should be stated that the strains for the two pixel density records was subjected to further analysis by fitting least-square straight lines through the data incorporating the origin. The 3.3 Mpixel data was represented by a proportionality between grip displacement and strain with a factor of 0.649 ($R^2=0.996$) and for the 5.2 Mpixel count by 0.669 ($R^2=0.988$); these fits represented a standard deviation from the straight lines of 0.99 for the lower pixel density and 0.188 for the higher one. Thus, the precision of the strains determined either way are precise to within one or two tenths of a percent.

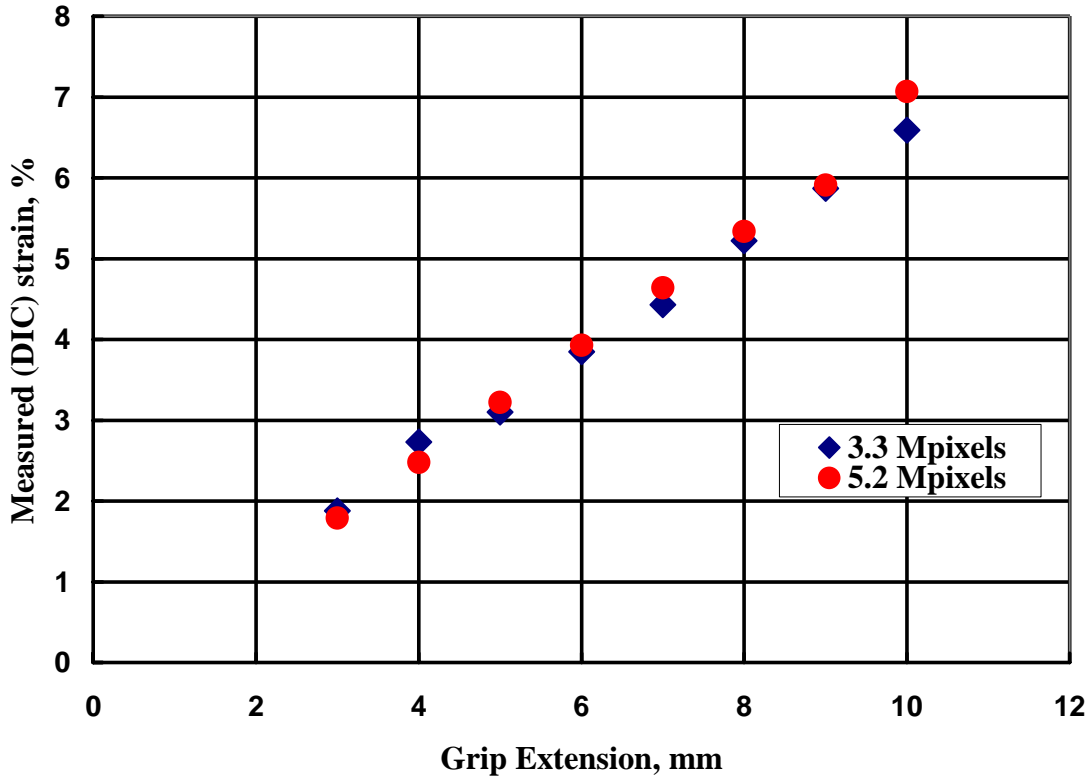


Figure 13: Comparison for DIC deduced strains with the aid of different camera image resolutions.

2.1.5 Temperature control and tracking

Temperature control was achieved via a Russel's environmental chamber (Model # RDB-3-LN2-33) employing a MICRISTAR controller (Model #828-D10-403-901-130-00). To reach temperatures below 0° C liquefied nitrogen was needed. At temperatures below -55 to 60 °C this cooling method became troublesome and rather expensive because of the large amount of liquid Nitrogen used.

A TestStar controller was used in conjunction with an OMEGA CN76000 Microprocessor-based Temperature/process controller and a type J Thermocouple located near the specimen inside the chamber. At low temperatures window frosting was a standard occurrence, but a fan heater kept the multi-pane window clear for optical (DIC-camera) access.

It was typically difficult with the existing equipment to predetermine the temperature precisely. This fact resulted from the restriction of the temperature controller and the long time scale required to achieve a prescribed temperature. Tests were thus conducted to assure a stable test temperature. These test runs established that a rather long time (hours) were required to have the temperature control chamber reach a constant temperature near

the desired value, and that the difference between the pre-set (“dialed-in”) value and the finally achieved one was not the same. Inasmuch as the precise pre-determination of the temperature was more a matter of convenience than a scientific constraint, it was decided that it was more important to reach a steady temperature rather than a particular, predetermined value. Correspondingly, the temperature was monitored continually in two ways: One was by means of the temperature record built into the test chamber, with the thermocouple near the entrance of the cooled or heated air. The other derived from an additional thermocouple placed close to the test specimen, the output of which was monitored continuously as a function of time. The two methods resulted in close agreement, and thus the output of the thermocouple that was placed close to the specimen was used for thermal definitions. As a result of this process the test results are reported for temperatures that are rarely integral values of temperature, but typically include fractional values

Temperatures were tracked continuously. In the early stages of the investigation relaxation data was rejected if the temperature variation was judged too large –in excess of $+\text{-}0.5^\circ\text{C}$. As test progressed that situation occurred less and less, so that the final data is essentially free of concerns in that direction. On the whole, analysis of the temperature history established that the standard deviation for temperatures in the steady state (long term tests) were on the order of $1/3^\circ\text{C}$.

2.2 Properties Determination

To minimize untoward and poorly understood nonlinear response an effort was made to prescribe sufficiently small deformations for the test sequences. This requirement supported the choice of large specimens so as to be able to prescribe strains accurately through machine controlled grip displacements. However, because failure would occur typically under “large” strains, a different specimen configuration was required that started with a shorter test section, so that the stroke of the machine was sufficient to impose failure strains at all temperatures considered.

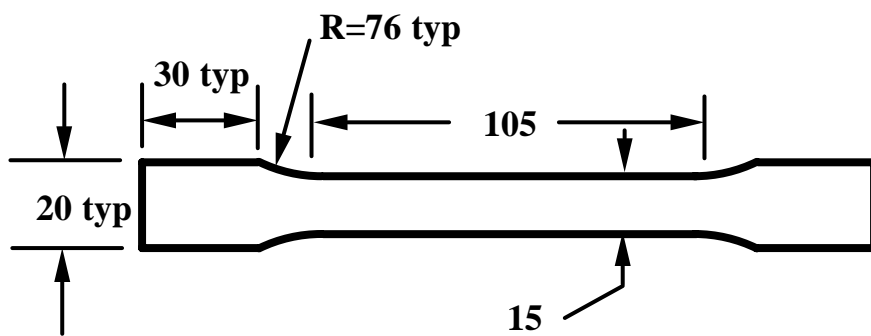


Figure 14: Specimen for relaxation tests. Dimensions are in mm, $+\text{-} 0.5$ mm. For cross sectional dimensions each specimen was measured separately.

2.2.1 Specimen configurations for relaxation and rupture tests.

The test specimen is illustrated in figure 14. Specimens were machined from nominally two mm thick sheet stock on an NC-milling machine with a 0.5 inch diameter, helically fluted cutter at 3600 rpm. The specimen was held in a fixture which guaranteed proper backing against the cutting force. The dimensions of each specimen were measured individually for properties evaluations. Specimens were used for measuring relaxation at different temperatures, but not more often than for five tests. In an initial evaluation aimed at ascertaining whether residual deformations or property changes were encountered upon repeated use gave erroneous messages, because the test machine provided inaccurate control (see elsewhere in this report). Upon correcting for this deficiency it was established that multiple use of the specimens was permissible at the strain levels encountered.

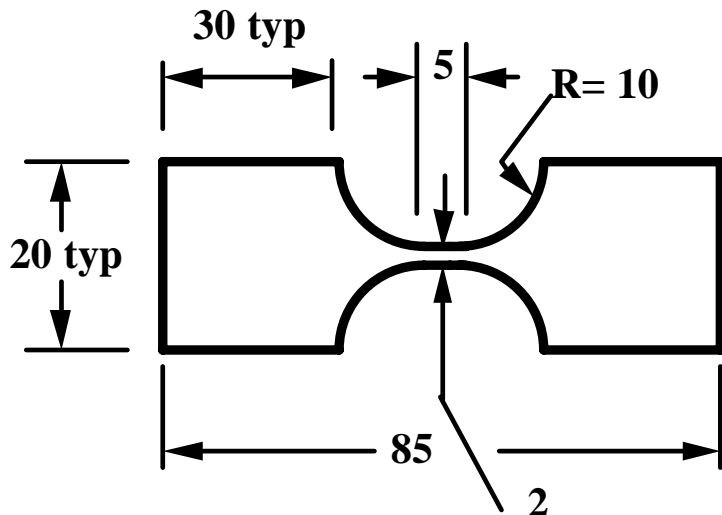


Figure 15: Specimen dimensions for failure tests, in mm, +/- 0.3 mm.
Each specimen was measured separately for each test.

2.2.2 Loading (straining) programs for relaxation

The MTS machine was programmed to strain the specimens in a ramp fashion, with the constant strain (displacement) being achieved in about a second. As a consequence of this time scale the data between 1 and 10 seconds was not considered, since it was too heavily flavored by the loading transient. Moreover, it was **not** deemed necessary to employ special methods to extract relaxation data from this short-time history, since the tests could be conducted for about a day each, thus rendering data in excess of three decades without even the first decade influenced by the loading transient.

2.2.4 Relaxation at various temperatures

Relaxation tests were thus conducted at various temperatures. The results are summarized in figure 16. Note that the ordinate represents the temperature-reduced scale, in preparation for the next step in the data reduction.

2.2.5 Master relaxation curve and time-temperature shift data

The data from figure 17 has been shifted according to the time-temperature shift principle. The result is shown in figure 18, along with the resulting shift factor in figures 19 and 20. We note first that the superposition fit of the temperature segments in figure 17 render a rather smoothly meshing set of curves that produces a distinct master curve. It is this quality of fitting/meshing that typically assures that applicability of the shift process. Next, note that the shift factor data in figure 19 is represented well by the (standard) WLF equation given by ($\Theta = \text{temperature, } {}^{\circ}\text{C}$)

$$\log a_T = -\frac{8.86(\Theta - 0.6)}{101.6 + (\Theta - 0.6)}. \quad (29)$$

Williams, Landel and Ferry established for about 50 polymers that the glass transition temperature is 50°C below the reference temperature, which is established here as -0.6 °C. It is clear by consulting figure xxx, that a variation of +/- 5 °C in the glass transition yields a readily distinguishable difference in the data fit. This value may differ by a small amount from a determination by differential scanning calorimetry (DSC), though that method has its own problems with being more precise.

2.2.6 Poisson Behavior

To deduce an estimate of the dilatational behavior an attempt was made to measure the time-dependent Poisson effect. It turned out that the DIC method was insufficiently accurate to a definitive statement about this behavior. While some test sequences resulted in the expected behavior of increasing Poisson number with time under relaxation, there were other tests in which the opposite or a constant behavior was observed. All measurements were close to (nearly) incompressible behavior with a contraction ratio of close to $\frac{1}{2}$ being observed. This kind of measurements is notoriously difficult, especially in the long-time or rubbery domain, where very small deviations from a value of $\frac{1}{2}$ leads to large variations in the bulk response.

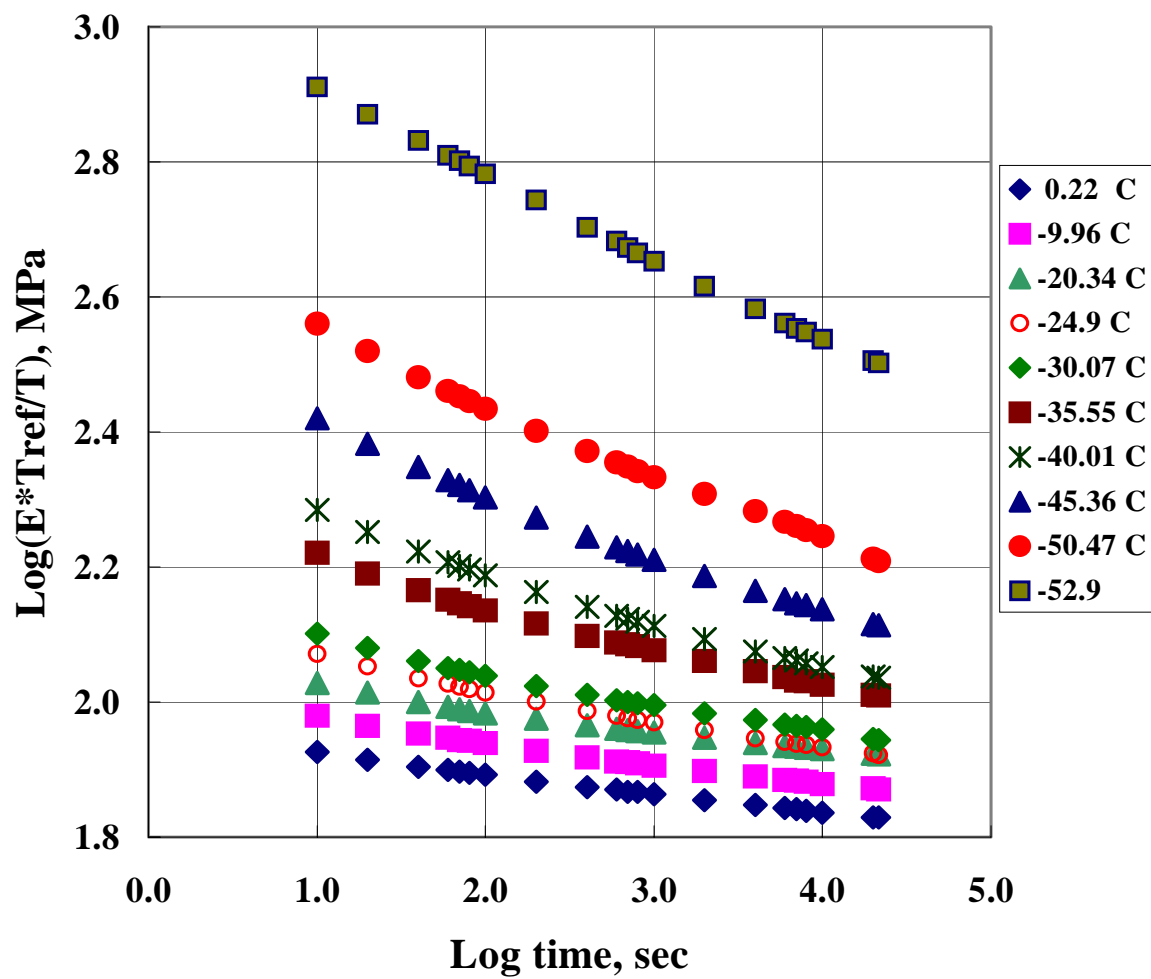


Figure 16: Relaxation response at various temperatures

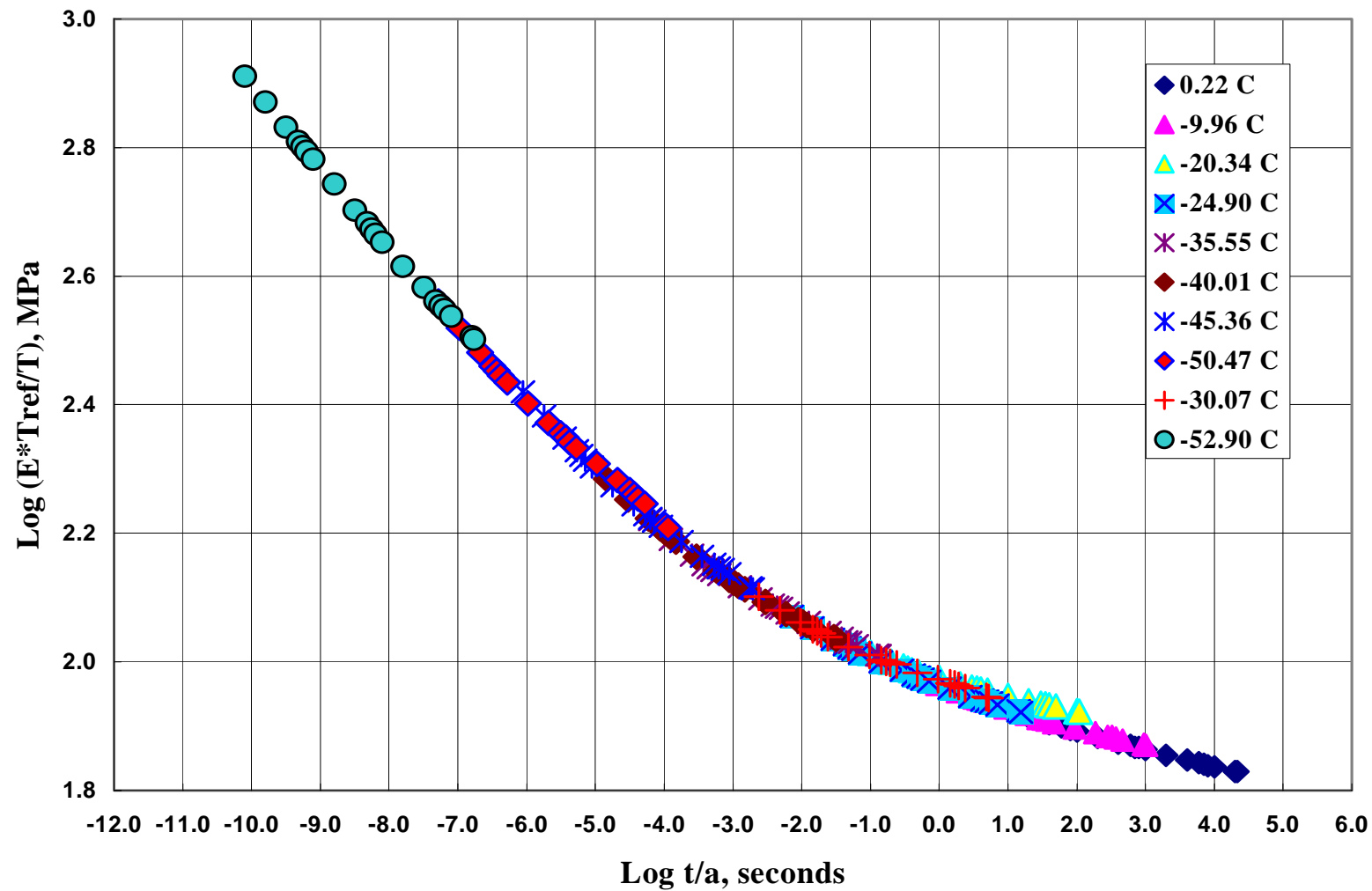


Figure 17: Master Relaxation Curve, referred to 0°C (0.22°C)

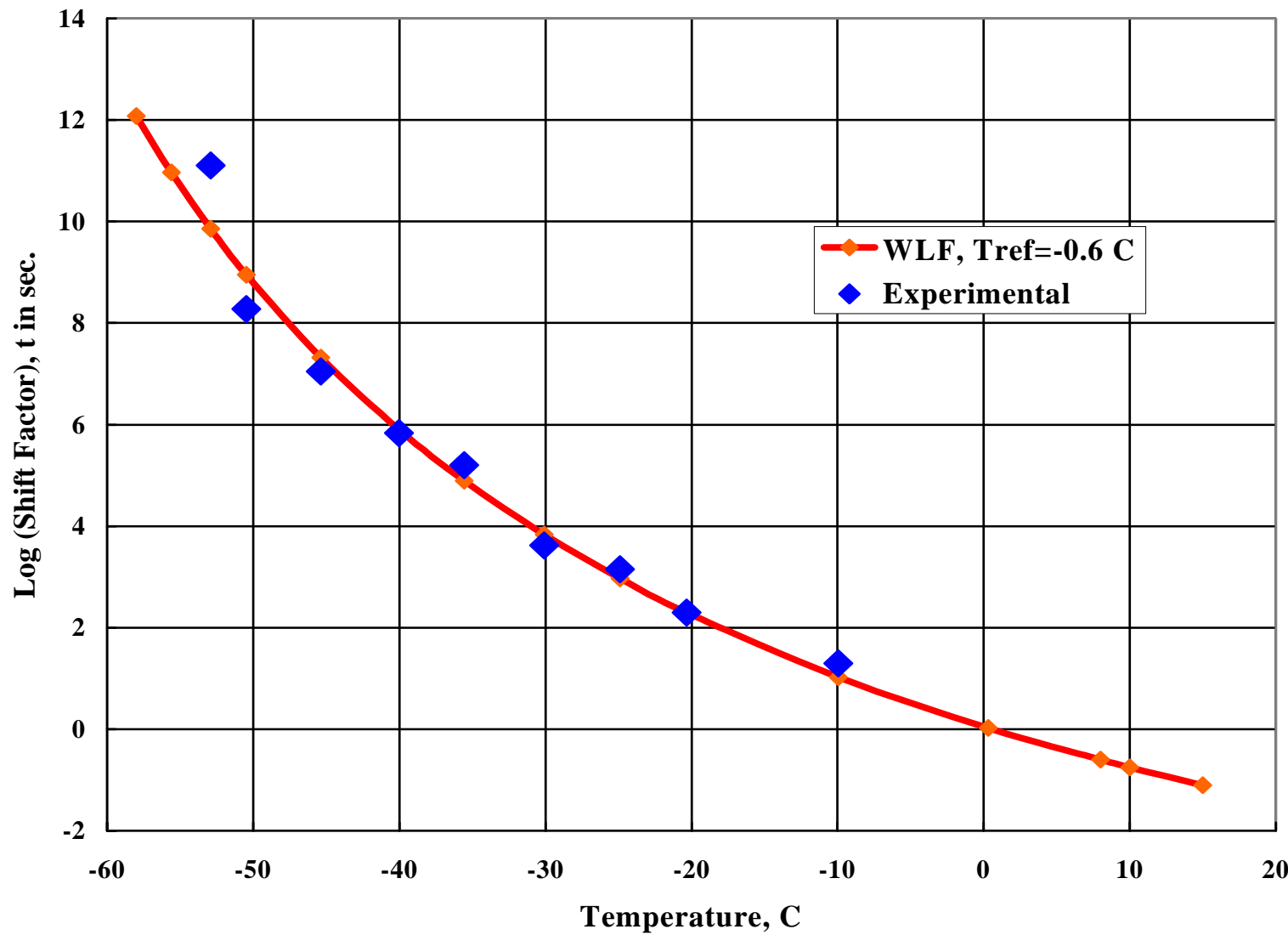


Figure 18. Shift factor data and fitted WLF equation (see text)
The glass transition temperature is about -50.6°C

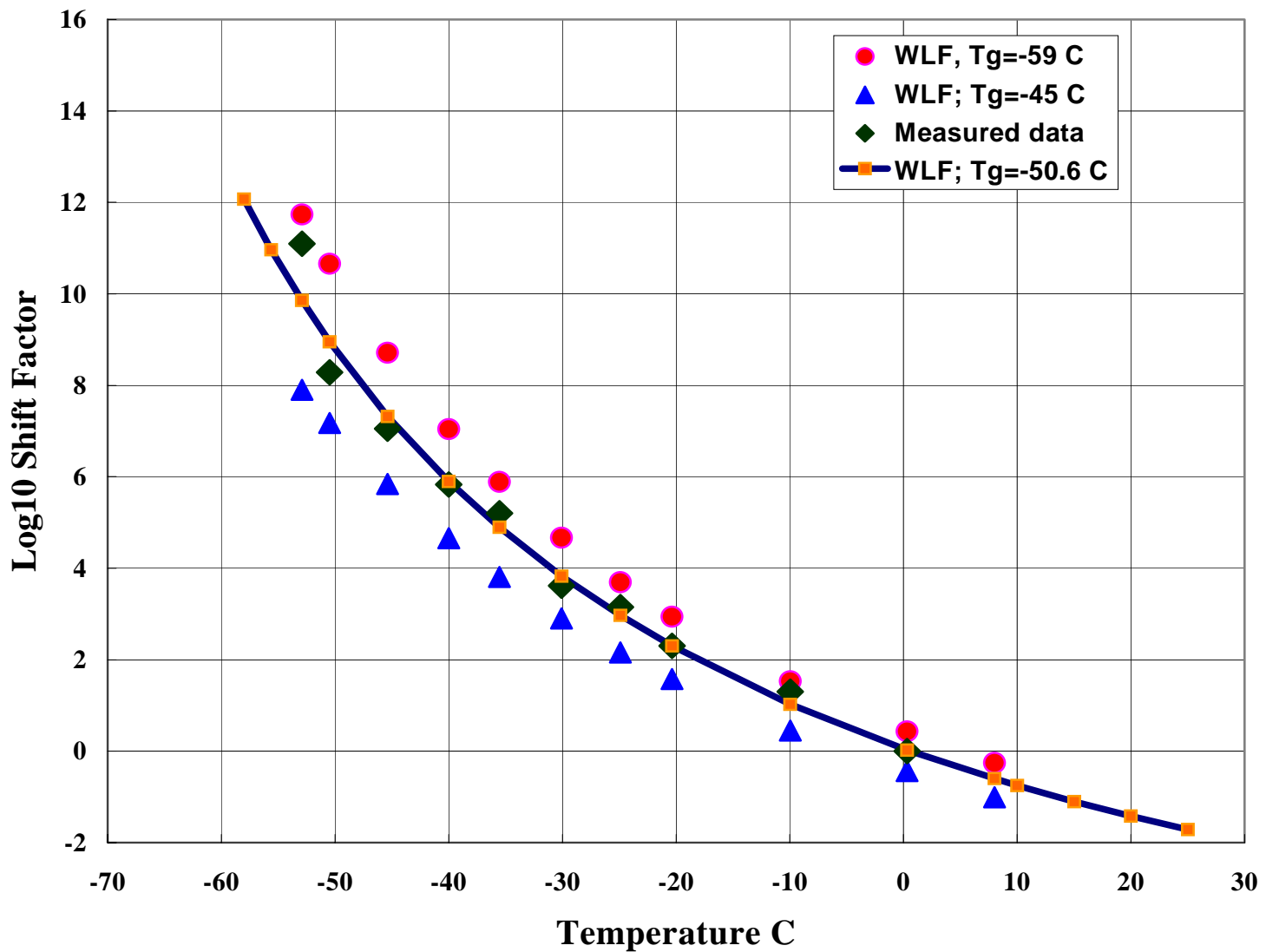


Figure 19: Shift Factor data compared with the WLF equation for three values of the glass transition temperature

2.2.7 Rupture Behavior

An important characteristic in engineering failure analyses are “properties” determined to assess the stress or strain capability of a material. The purpose of such measurements is typically to bound the capability of the material or to establish “allowable” quantities. Most often this is effected through uniaxial tensile testing, though compression testing is also of importance in appropriate engineering situations. Just to illustrate the effect of rate of deformation (and temperature by way of the time-temperature-tradeoff Principle) on such allowables as the ultimate stress and/or strain achieved in uniaxial tensile tests under constant rate of deformation are presented here. Considerably different values are achieved depending on the time scale involved in the measurements (rate $\approx t^{-1}$).

2.2.6.1 *Definition of an equivalent constant strain rate.*

Failure strain determination requires a specimen (*cf.* figure 15) that allows failure to occur away from stress concentration caused by the grips of the test machine. The resulting inhomogeneity of the specimen straining leads to a (large) strain that is not proportional to the grip motion. Figure 20 shows a typical example of a test result, with the measured values of the strain across benchmarks denoted on the specimens. These measurements were conducted near room temperature (23 °C) where relaxation plays a minor role, though the latter has no influence on the geometric effects incorporated the results shown in figure 21. Clearly the behavior is anything but linear. To establish a quasi-constant strain rate, we replace the true strain curve by a least square fit by a constant-slope line to define a (constant) strain rate. This is roughly justified inasmuch as the viscoelastic response is really sensitive to the **logarithm** of the strain rates, rather than relatively small variations of that quantity.

The next figure shows a typical trace of the nominal (engineering) stress as a function of the applied strain. The rise in the stress at elevated strain (~200 to 400 %) arises from the molecular orientation typical of high strain elastomer behavior.

2.2.6.2 *Results for uniaxial failure.*

Two measures for failure were considered, namely ultimate strain and ultimate stress. In the following figures strain is given in terms of engineering values, *i.e.* $(l-l_0)/l_0$, and not in percent values. Stresses are given in terms of the engineering stress as well as in terms of true stress, which was deduced from the extension and the lateral contraction based on volume constancy. This was used regardless of the test temperature. The strain rate (abscissa) is computed for the three nominal strain rates at different temperatures. However, the strain rates have been converted to effective values according to the time-temperature trade-off principle represented in figure 18.

One notes that the maximum strain (Figure 24) remains on the order of 3 (300%), though there is a small trend to decreased strain capability as higher effective strain rates are encountered.

The stresses, on the other hand, appear to pass through a maximum at a strain rate of 10^4 per sec, with a local minimum at 10^6 per sec. this holds true for the engineering and for the true stress. The three strain rates used in the tests give rise to a systematic shift to higher rates as one passes from 5 to 50 mm/sec rates. However, the stress amplitudes vary considerably; experience would indicate that this result derives, in good portion, from micro fractures incurred in the specimen machining process.

As a minimum, these data provide a set for response bounds on the material in engineering applications.

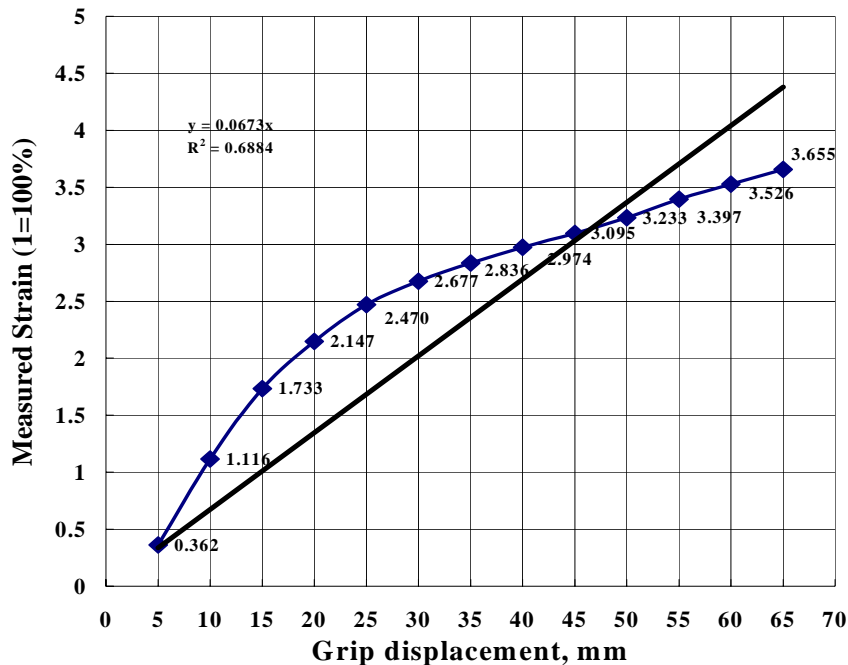


**Figure 20: Definition of an equivalent strain rate.
Strain measured in the test section of the specimen.**

2.2.8 *The influence of Pressure on time dependent behavior*

In section 1.1.6 it was observed that pressure has a notable influence on the relaxation times of a viscoelastic polymer, similar to the influence of temperature: Higher pressure changes the internal time scale (relaxation times) to longer times similar to cooling the material. The only direct experimental study of this effect has been supplied by Fillers and Tschoegl (1977), and by Moonan and Tschoegl (1985).

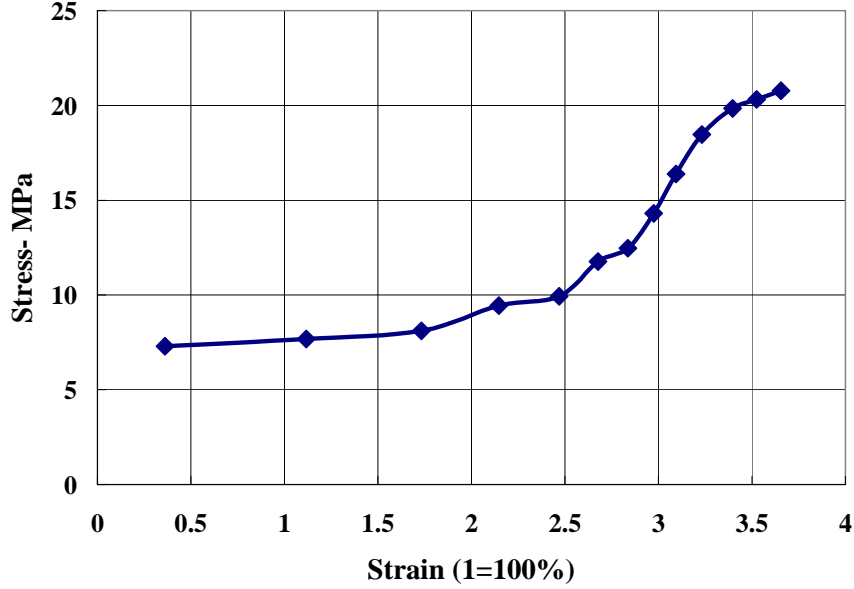


Figure 21: Example of an engineering (nominal) stress-strain response. Note the stiffening of the material at higher strains (molecular orientation and toughening)

The effect of changing pressure and temperature is included through the concept to the *intrinsic material time* defined, for a change in pressure and temperature to other constant values by

$$t' = \frac{t}{a_{T,P}}. \quad (30)$$

If changes in pressure and/or temperature occur continuously, this relation applies instantaneously so that as a function of any pressure or temperature history one finds the pressure/temperature reduced time from

$$t' = \int_0^t \frac{dt}{a_{T,P}}. \quad (31)$$

In these equations the shift factor is given by

$$a_{T,P} = a_{T,P}[T(t), P(t)] \quad (32)$$

and in detail by

$$\log(a_{T,P}) = -\frac{c_1[T - T_0 - \theta(P)]}{c_2 + T - T_0 - \theta(P)} \quad (33)$$

where the function $\theta(P)$ is

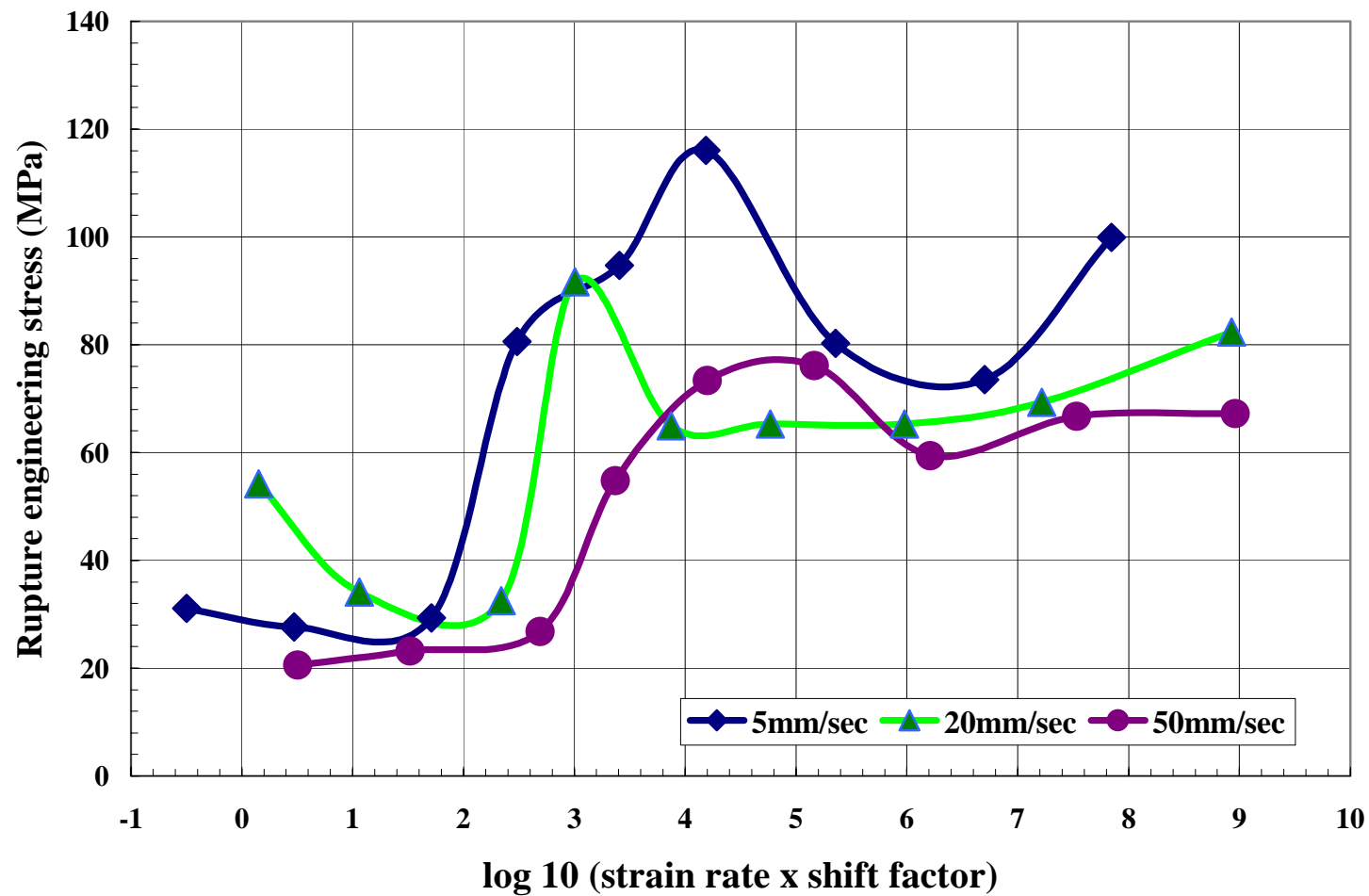


Figure 22: Rupture engineering stress as a function of the rate of deformation

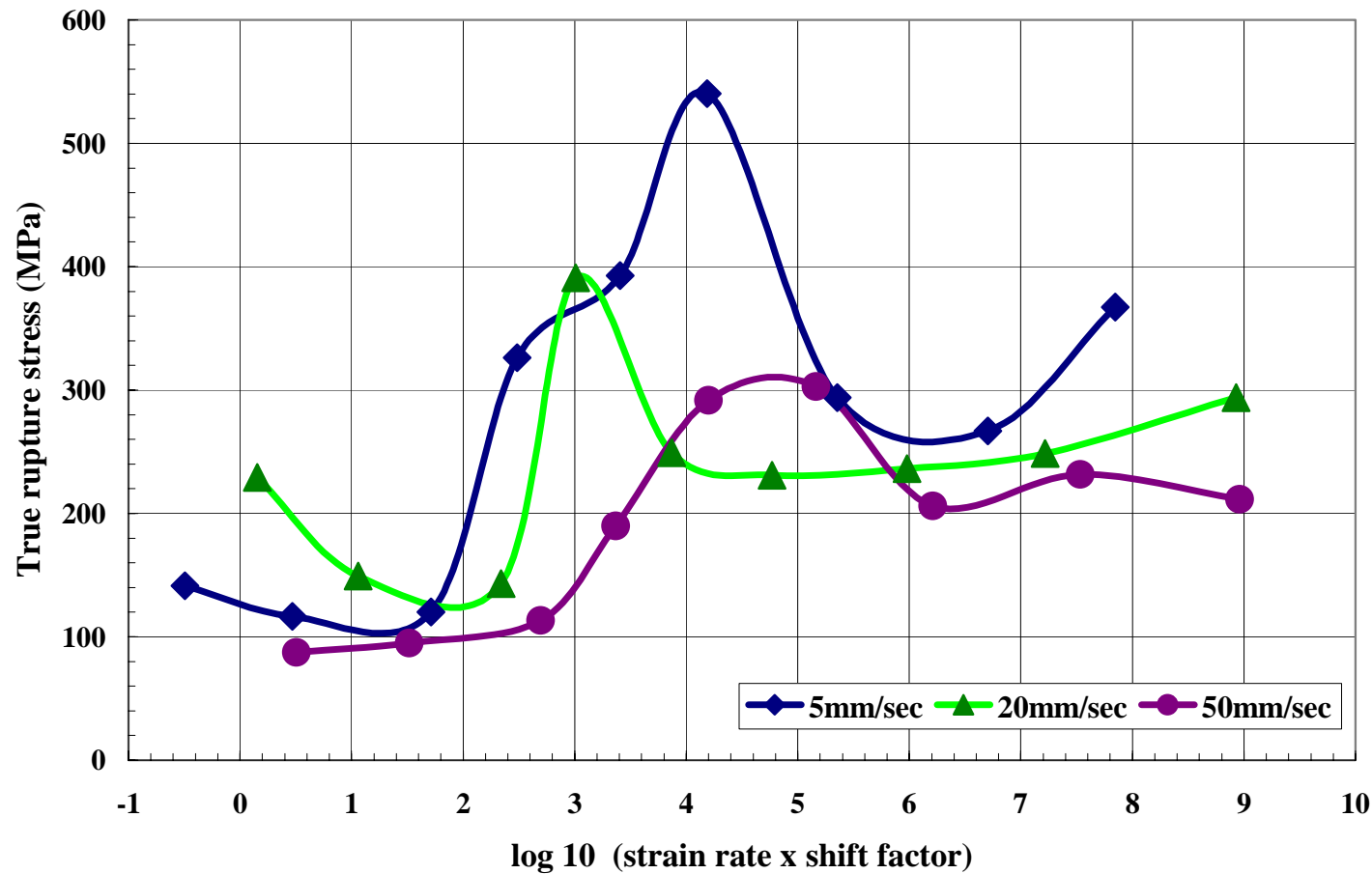


Figure 23: True rupture stress as a function of the rate of deformation.

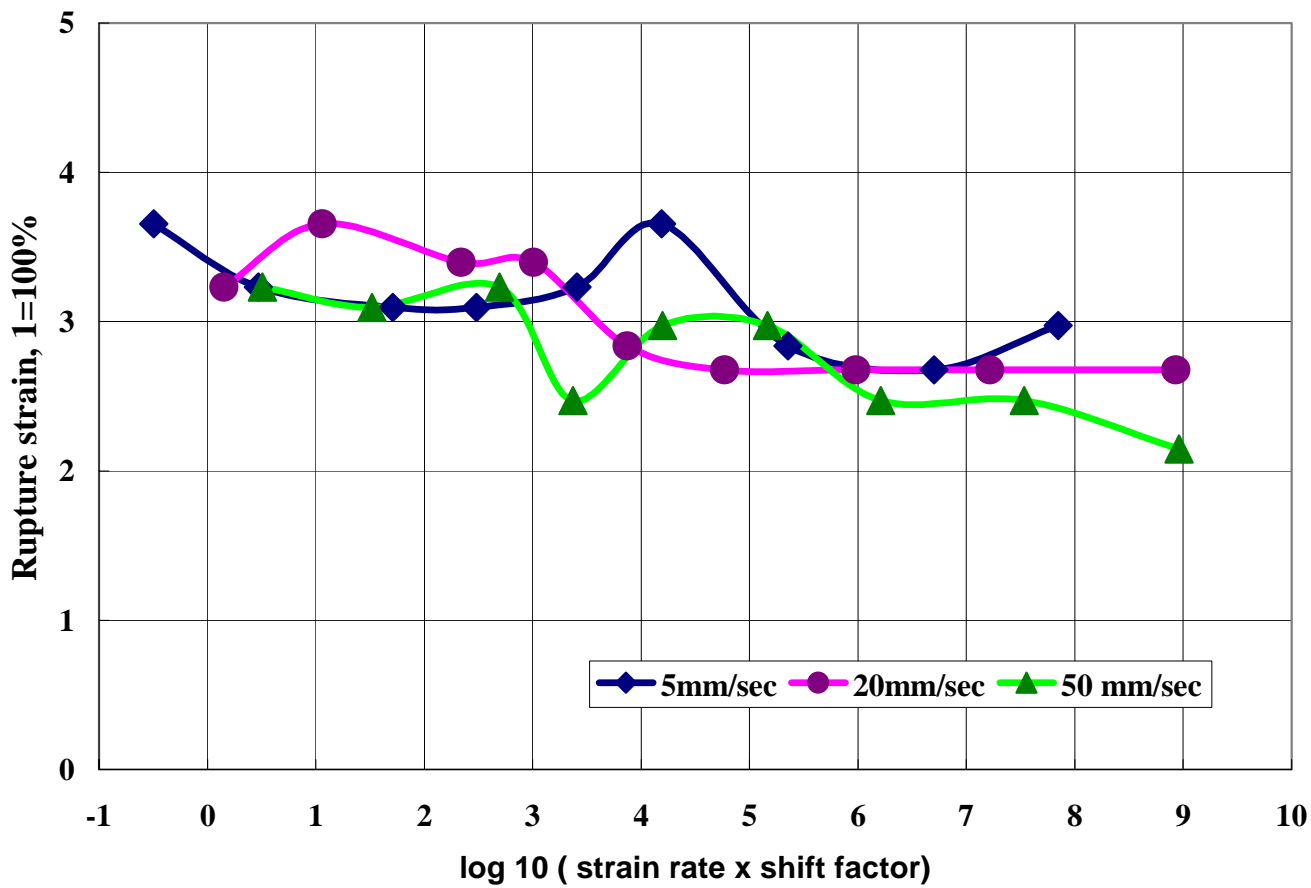


Figure 24: Rupture strain as a function of deformation rate

$$\theta(P) = c_3 \ln\left[\frac{1+c_4P}{1+c_4P_0}\right] - c_5 \ln\left[\frac{1+c_6P}{1+c_6P_0}\right] \quad (34)$$

where P is measured in kbars and the constants c_i are, for example, for Hypalon 40, one of the materials studied by Fillers and Tschoegl (1977), $c_1=2.66$, $c_2=60.0$, $c_3=152.0$, $c_4=0.526$, $c_5=105.8$, $c_6=0.576$; similarly it was found that $c_1=2.24$, $c_2=59.4$, $c_3=145.6$, $c_4=0.402$, $c_5=69.4$, $c_6=0.395$ for Viton B. For more detailed information the reader is referred to the publications by Tschoegl and his coworkers.

It bears mentioning that since c_4 and c_6 are less than unity so that for small pressures the relation is basically linear in the pressure. However once pressures exceed several kbars that is no longer the case, though the nonlinearity is "mild".

2.2.8.1 Examples of pressure shifting

Consider three examples to show the effect of pressure in terms of the isothermal pressure shift factor in figures 25,26 and 27.

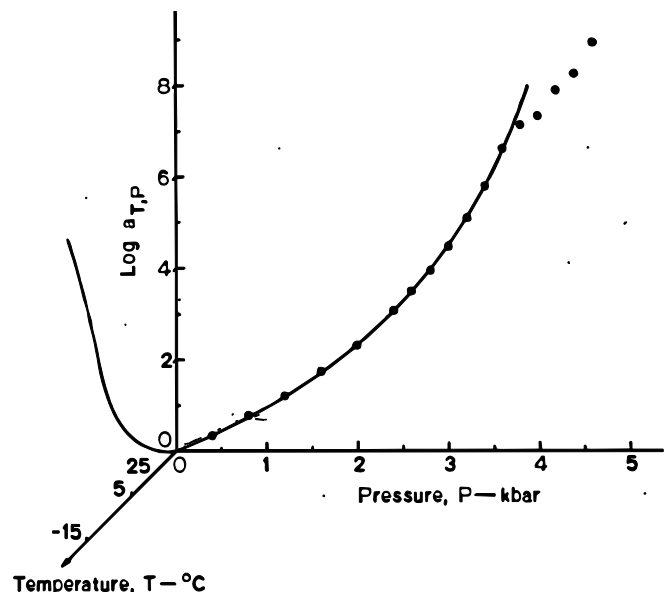


**Figure 25: Pressure shift factor for Hypalon 40.
(Reference temperature 25 °C, and pressure at 1 bar
Fillers and Tschoegl, 1977)**

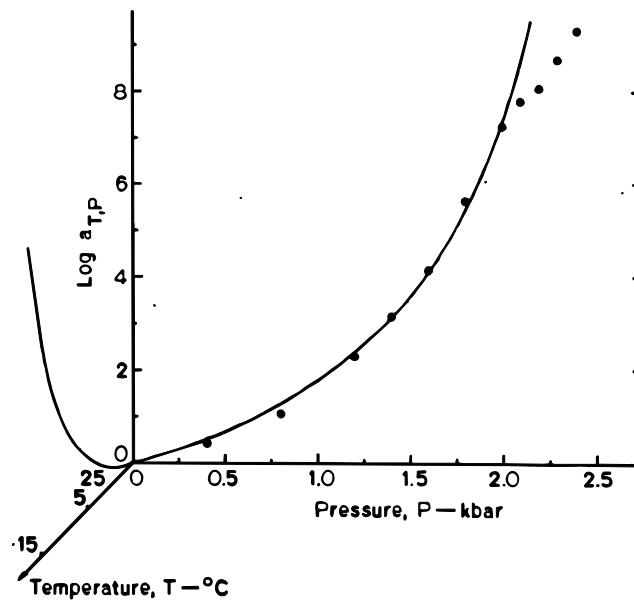


**Figure 26: Pressure shift factor for Viton B.
(Reference temperature 25 °C, and pressure at 1 bar
Fillers and Tschoegl, 1977)**

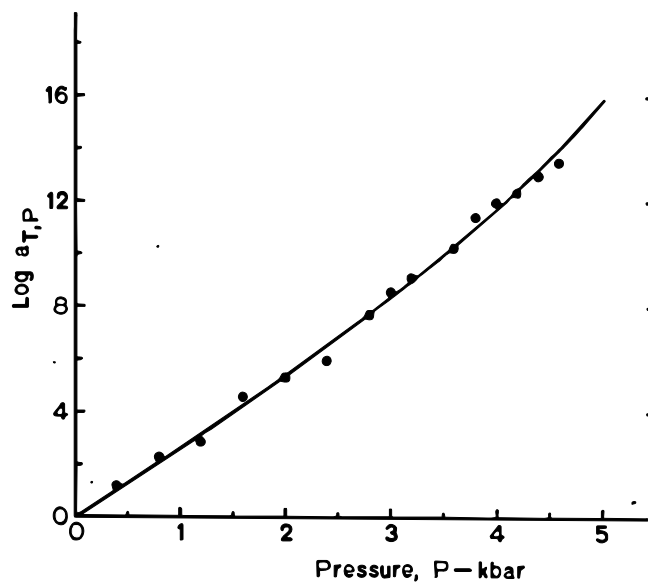


**Figure 27: Pressure shift factor for Neoprene WB.
(Reference temperature 25 °C, and pressure at 1 bar
Fillers and Tschoegl, 1977)**

These three rubbery materials provide numerical estimates of how much the time scale changes as a result of pressure (in kbars). This is summarized in Table II

	P = 2 kbar	P = 4 kbar
Hypalon 40	2.5	8
Viton B	7	-
Neoprene WB	5	11

Table II: Shift factors for pressure increases for three elastomers

It is apparent that very significant stiffening can result in a high pressure environment. To the best of our knowledge, this response is valid under isostatic as well as dynamically changing conditions. In the latter case it would be necessary, in principle, to prescribe a specific pressure history and execute the integration in equation (31-33) to evaluate elastomer “stiffness” in connection with the constitutive law outlined for small strains in equation (23-24 and sequel). Just to keep matters in perspective, recall that in the material examined in the present work, that a shift of 8 decades to longer times (stiffening) arises from a lowering of the temperature by about 50 °C, which brings the material close to, if not directly to, the glass transition temperature. Thus under high pressures the material responds highly viscously or in a leathery manner.

2.2.8.2 *Need for data for subsequent analyses.*

To date the above referenced data are virtually the only ones available, or certainly the most complete. More recent work by Qvale and Ravi-Chandar (2004, see section 1.1.6) is more limited, but points in the same direction.

What is most important in the present characterization effort is to recognize that both the pressurization process as well as the high rate (short time scale) leads **additively** to material “stiffening” which corresponds to a time scale that is not covered by the measurements in this report.

3. APPLICATION TO ARBITRARY TEMPERATURES AND DEFORMATION HISTORIES

The most immediate question relates to the interpretation of the relaxation modulus in figure 17 when a use temperature different from the reference temperature of ~0 °C us of interest. Assuming that the application of this material is at 15 °C, the master curve of figure 17 has been replotted in figure 28; this amounted to shifting the curve to shorter log-times by an amount of 1.074 logarithmic units which corresponds to the time

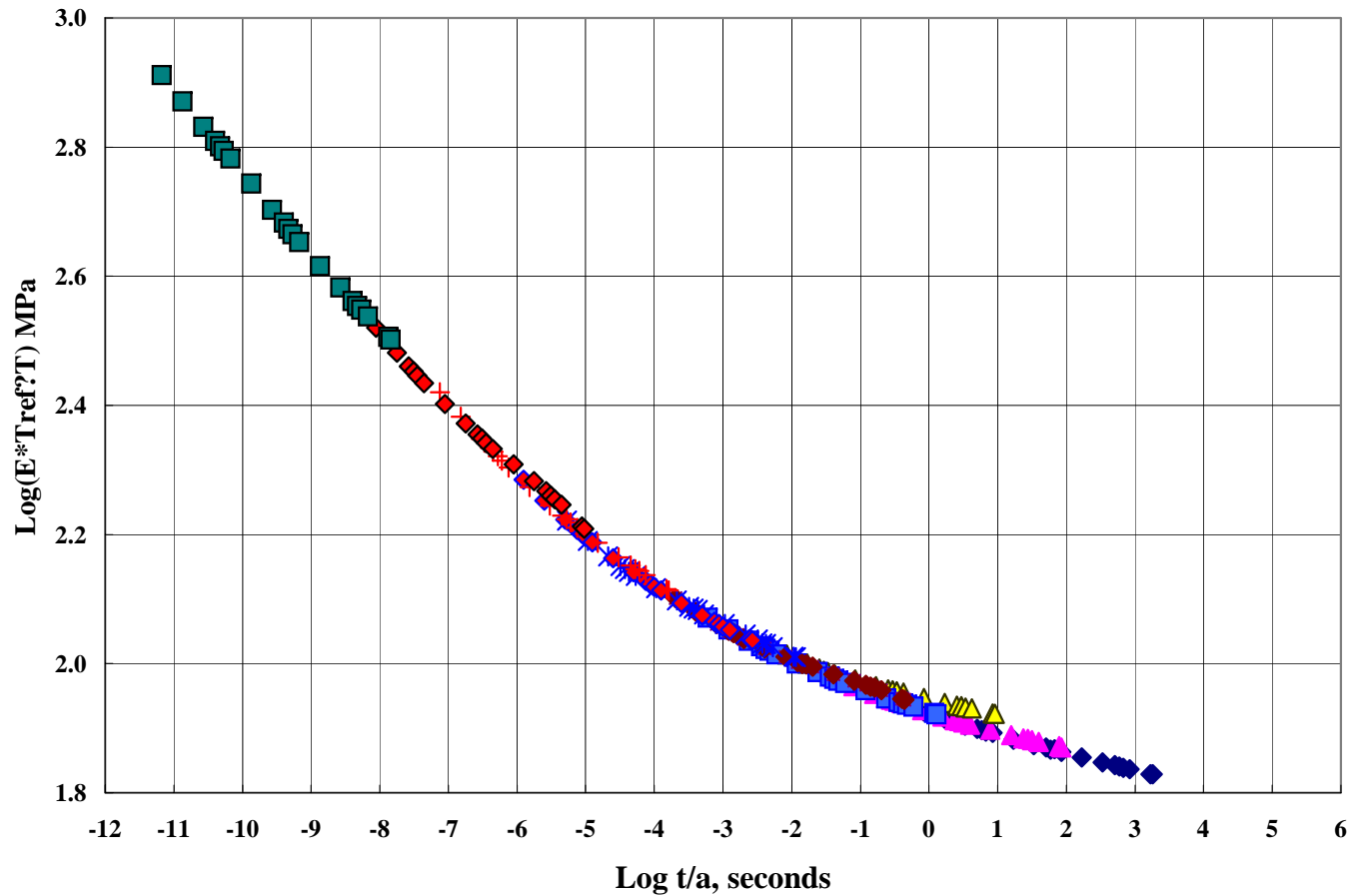


Figure 28: Relaxation modulus at 15 °C. (The ordinate adjustment from figure 17 is only 5%; on a log scale this means a change of 2% and has not been added)

temperature shift computed from the WLF equation (). Because the ratio of the absolute temperature for 15 °C and the reference temperature is 278/273 is small, the adjustment of the data along the (logarithmic) ordinate is very small and has not been incorporated into that figure.

3.1 VARIABLE TEMPERATURE AND PRESSURE

We recall the three-dimensional equations of (linear) viscoelasticity

$$S_{ij}(\mathbf{x}, t) = \int_0^t \mu(t' - \xi') \frac{\partial e_{ij}(\mathbf{x}, \xi)}{\partial \xi} d\xi \quad (35)$$

$$\tau_{ii}(\mathbf{x}, t) = 3 \int_0^t k(t' - \xi') \frac{\partial [e(\mathbf{x}, \xi) - \alpha \Delta T(\mathbf{x}, \xi)]}{\partial \xi} d\xi \quad (36)$$

as well as the definitions of the temperature/pressure reduced time(s)

$$t' = \int_0^t \frac{dt}{a_{T,P}}. \quad (37)$$

$$\xi' = \int_0^{\xi} \frac{dt}{a_{T,P}}. \quad (38)$$

$$\text{or} \quad t' - \xi' = \int_{\xi}^t \frac{dt}{a_{T,P}} \quad (39)$$

with the shift factor $a_{T,P}$ is given by equations (33) and (34).

3.2 APPROXIMATIONS FOR FINITE DEFORMATIONS.

While there are numerous formulation issues associated with large deformations, the primary question in the present context arises with regard to interpretation of the nonlinear behavior in the uniaxial data. While an initial approach would be to follow the free volume concept offered by Knauss and Emri (1981, 1987), or the stress-induced nonlinear approach discussed by Schapery (1968, 1969), these concepts reduce, in the limit of near-rubber behavior (long-time response) to a multiplicative decomposition into the viscoelastic component and a nonlinear strain function as long as the deformation follows a constant rate history.

Discussing this in terms of uniaxial behavior would yield with $\varepsilon_{11}=R \cdot t$, as a simple approximation

$$\sigma_{11}(t) = f(\varepsilon_{11})R \int_0^t E(t-\xi)d\xi \quad (40)$$

where $f(\varepsilon_{11})$ is an experimentally determined function. This relation states simply that the time dependencies summarized in the viscoelastic integral, and the strain dependence in the function f . If one defines the viscoelastic secant modulus or constant rate modulus $E_R(t)$ as

$$E_R(t) = \frac{1}{t} \int_0^t E(t-\xi)d\xi \quad (41)$$

then (41) may be written, upon noting that $\varepsilon_{11} = Rt$, as

$$\sigma_{11}(t) = f(\varepsilon_{11}) \cdot [\varepsilon_{11} \cdot E_R(t)] \quad (42)$$

This relation may be used to correlate constant strain rate (constant deformation rate) data as obtained from Instron or MTS instruments. Note that the quantity in brackets represents the linearly viscoelastic response in a uniaxial, constant strain rate test, such as would be computed from the relaxation data in figure 17 or 28.

3.3 APPROXIMATIONS FOR MONOTONICALLY CHANGING DEFORMATIONS

The following is a simple method for estimating stress and deformations in complex situations. It gives erroneous results if cyclical deformations are involved, or if rates change sign. The crux of the method is to determine a reasonably good estimate for the material stiffness. This value is governed by the temperature (history), pressure (history) and deformation rate. If deformations remain small, in if rates are monotonic, a decent approximation for the stiffness of the material is obtained by the following process:

- develop the relaxation master curve for the appropriate temperature (and pressure);
- determine the time scale of interest; if the deformation is continuous choose the final time; if relaxation is involved, choose the final time.
- Determine the modulus for the time chosen; this value is a reasonable first estimate for stress and deformation analysis.

The reason that this method is useful is that the modulus changes significantly only if deformation rates change by an order of magnitude: it is a modulus that is relatively insensitive to details of the deformation history (which is determined by way of an integral)

The results of such a computation renders the right order of magnitude of quantities, and is probably within +/- 15 % of the desired linearly viscoelastic result.

4. *References*

Christensen, R.M., 1971, "Theory of Viscoelasticity, An Introduction". *Academic Press*. See also: Christensen, R.M. 1982, "Theory of Viscoelasticity, Second Edition". *Dover Publications*.

Fillers, R.W. and Tschoegl, N.W., 1977, "The Effect of Pressure on the Mechanical Properties of Polymers", *Trans.Soc. Rheol.*, **21**, 51-100.

Knauss, W.G. and Emri, 1981, I.; "Non-Linear Viscoelasticity Based on Free Volume Consideration", *Computers & Structures*, **13**, pp. 123-128.

Knauss, W.G. and Emri, I. 1987; "Volume Change and the Nonlinearly Thermo-Viscoelastic Constitution of Polymers", *Polymer Engineering and Science*, A. Yee (ed.), **27**, pp. 86-100.

Knauss, W.G., Zhu W., "Nonlinearly Viscoelastic Behavior of Polycarbonate"

- I. Response Under Pure Shear. *Mechanics of Time Dependent Materials*, **6**, No.3, pp 207-229, 2002
- II. The Role of Volumetric Strain., *Mechanics of Time Dependent Materials*, **7**, No. 4, pp231-269, 2003

Losi, G.U. and Knauss, W.G., 1992, "Free Volume Theory and Nonlinear Thermoviscoelasticity", *Polymer Engineering and Science*, **32**, (8), pp. 542-557.

Lu, H. and Knauss, W.G., 1999; "The Role of Dilatation in the Nonlinearly Viscoelastic Behavior of PMMA under Multiaxial Stress States", *Mechanics of Time-Dependent Materials*, **2**, (4), pp. 307-334.

Moonan, W.K. and Tschoegl, N.W., 1885, "The Effect of Pressure on the Mechanical Properties of Polymers. IV. Measurements in Torsion," *J. Polym. Sci., Polym. Phys.Ed.*, **23**, 623-651.

Plazek, D.J., 1965, "Temperature Dependence of the Viscoelastic Behavior of Polystyrene. *J. Phys. Chem.*, **69**, P. 3480.

Qvale and Ravi-Chandar, 2004, " Viscoelastic Characterization of Polymers under Multiaxial Compression", to appear in *Mechanics of Time Dependent Materials* **8**.

Schapery, R.A., 1968, "On a Thermodynamic Constitutive Theory and Its Application to Various Nonlinear Materials", *Proceedings of the IUTAM Symposium East Kilbride*.

Schapery, R.A., 1969, "On the Characterization of Nonlinear Viscoelastic Materials", *Polymer Engineering and Science*, **9**, No.4.

Tschoegl, N.W., Knauss W.G., Emri I., 2001, "The Effect of Temperature and Pressure on the Mechanical Properties of Thermo-and /or Piezorheologically Simple Polymeric Materials in Thermodynamic Equilibrium-A Critical Review. *Mechanics of Time-Dependent Materials*, **5**, (2)

Treloar, L.R. G., 1958, "The Physics of Rubber Elasticity." *Oxford at the Clarendon Press.*

Williams, M.L., Landel, R.F. and Ferry, J.D., 1955, " The temperature dependence of relaxation mechanisms in amorphous polymers and other glass-forming liquids". *J. Am. Chem. Soc.*,**77**, pp. 3701-3707

5. Acknowledgements

The PI is very grateful to Mr. M. Raz of RAFAEL, Israel, for his devoted participation in the measurements and data reduction phase of this work. Without his assistance this study would not have been possible.